View metadata, citation and similar papers at core.ac.uk

brought to you by CORE

provided by NASA Technical Reports Server

NASA
TP
1569
c.1

NASA Technical Paper 1569

TECH LIBRARY KAFB, NM
0134776

Wear, Friction, and Temperature Characteristics of an Aircraft Tire Undergoing Braking and Cornering

John L. McCarty, Thomas J. Yager,
and S. R. Riccitiello

DECEMBER 1979

NASA

TECH LIBRARY KAFB, NM
0134776

NASA Technical Paper 1569

Wear, Friction, and Temperature Characteristics of an Aircraft Tire Undergoing Braking and Cornering

John L. McCarty and Thomas J. Yager
Langley Research Center
Hampton, Virginia

S. R. Riccitiello
Ames Research Center
Moffett Field, California

National Aeronautics
and Space Administration

**Scientific and Technical
Information Branch**

1979

SUMMARY

An experimental investigation was conducted to evaluate the wear, friction, and temperature characteristics of aircraft tire treads fabricated from different elastomers. Braking and cornering tests were performed on size 22 × 5.5, type VII aircraft tires retreaded with currently employed and experimental elastomers. The braking tests consisted of gearing the tire to a driving wheel of a ground vehicle to provide operations at fixed slip ratios on dry surfaces of smooth and coarse asphalt and concrete. The cornering tests involved freely rolling the tire at fixed yaw angles of 0^{o} to 24^{o} on the dry smooth asphalt surface. The results show that the cumulative tread wear varies linearly with distance traveled at all slip ratios and yaw angles. The wear rate increases with increasing slip ratio during braking and increasing yaw angle during cornering. The extent of wear in either operational mode is influenced by the character of the runway surface. Of the four tread elastomers investigated, 100-percent natural rubber was shown to be the least wear resistant and the state-of-the-art elastomer, comprised of a 75/25 polyblend of cis-polyisoprene and cis-polybutadiene, proved most resistant to wear. The results also show that the tread surface temperature and the friction coefficient developed during braking and cornering is independent of the tread elastomer. A comparison of tire-tread data obtained during the cornering tests with those from the braking tests, on the basis of equivalent slip velocities, suggests that the amount of tread wear is comparable but friction and surface temperatures are greater during braking operations. The difference is attributed to the tire being softer in the lateral direction which would tend to reduce the relative slippage between the tire and the pavement and therefore provide a lower effective slip ratio in cornering.

INTRODUCTION

Tire replacement is of major economic concern to the aviation industry. The reasons for tire replacement include cutting, which is generally attributed to characteristics of the runway surface and to the presence of foreign objects; tearing and chunking, where strips or chunks of rubber are separated from the tire; and tread wear, which results from braking, yawed rolling maneuvers, and wheel spin-up at touchdown. The primary reason is tread wear, particularly that due to the braking and yawed rolling required during the landing roll-out and taxi phases of the normal ground operations of an airplane. In view of the economic and inherent safety considerations, NASA undertook a program in the early 1970's to examine the effects of tire tread wear attributed to the various ground operations of an airplane. Reference 1 presents the results from the initial study which explored the wear and related characteristics of friction and tread surface temperatures for an aircraft tire during braking. The purpose of the investigation reported in this paper is to extend that initial study (ref. 1) to include (1) different tread materials with known elastomeric composition, (2) different runway surfaces, (3) more complete temperature coverage both on and beneath the tread surface, (4) higher slip ratios in the

braking mode, and (5) operations in the yawed rolling mode. The tires for this study were size 22 × 5.5, type VII aircraft tires retreaded with both currently employed and experimental elastomers. The experimental elastomers are part of a program being conducted by the Chemical Research Projects Office at the NASA Ames Research Center to seek new elastomeric materials which would provide improved tire tread wear, traction, and blowout resistance. This program and some of the early test results are discussed in reference 2.

SYMBOLS

Values are given in both SI and U.S. Customary Units. The measurements and calculations were made in U.S. Customary Units.

N_b number of revolutions of braked wheel over a measured distance

N_o number of revolutions of free-rolling (unbraked) unyawed wheel over a measured distance

N_ψ number of revolutions of free-rolling yawed wheel over a measured distance

R_s slip ratio

V_g test speed of ground vehicle

V_t tire circumferential velocity

$V_{r,b}$ resultant slip velocity of a braked, unyawed tire

$V_{r,\psi}$ resultant slip velocity of a free-rolling yawed tire

ψ yaw angle

APPARATUS AND TEST PROCEDURE

Tires

The tires of this investigation were size 22 × 5.5, 12-ply rating, type VII, aircraft tires which were retreaded with stocks which used the four different elastomers defined in the following table:

Elastomer	Composition
A	100% natural rubber
B	75% rubber (85% natural, 15% synthetic) 25% cis-polybutadiene
C	75% natural rubber 25% vinyl polybutadiene
D	75% natural rubber 25% trans polypentenemer

Elastomer A was selected for testing because natural rubber has been considered the elastomer that would best satisfy the tire requirements for supersonic transport-type aircraft. State-of-the-art treads for jet transports are typically comprised of a 75/25 polyblend of cis-polyisoprene, either as natural rubber or "synthetic" natural rubber, and cis-polybutadiene. One such tread stock, in an optimized formulation developed to satisfy various airline carrier requirements, is identified in the table as elastomer B. Elastomers C and D were experimental and the formulation of the tread stock from those materials was not optimized. All retreads were cured in the same mold; thus, all tires had an identical tread pattern of three circumferential grooves. During the retreading process, half of the tires were equipped with two thermocouples each, which were installed on the same shoulder of the carcass beneath the tread. The purpose of these thermocouples was to measure the hysteretic heating within the carcass of the tire at a location where tire flexing is great. For all tests, the tires were vertically loaded to 17.8 kN (4000 lb) which was the approximate maximum loading available with the test fixture and somewhat below the rated loading of 31.6 kN (7100 lb) for this tire size. The tire inflation pressure for all but one test was reduced from the rated 1620 kPa (235 psi) to 738 kPa (107 psi), the pressure necessary to produce a 30-percent tire deflection under the test loading. Wear, friction, and temperature data were obtained for each of the fixed-slip-ratio conditions, generally throughout the life of each tire tread, that is, until most of the tread rubber was removed. In several of these tests, one tire was used to provide data for two test conditions because of the limited number of available tires.

Test Surfaces

The fixed-slip-ratio tests were conducted on one concrete and two asphalt surfaces at the NASA Wallops Flight Center. Close-up photographs of the surfaces are presented in figure 1. The surface identified as coarse asphalt had an average texture depth of 0.39 mm (0.0152 in.) as measured by the grease technique described in reference 3. The texture depth of the smooth asphalt averaged 0.27 mm (0.0104 in.). The concrete had the lowest average texture depth (0.24 mm (0.009 in.)) but had a very abrasive sandpaperlike surface. All tire yaw tests were conducted only on the smooth asphalt. Both the fixed-slip ratio and the yaw tests were performed with the surfaces dry.

Ground Test Vehicle and Instrumentation

Figure 2 is a photograph of the powered ground test vehicle employed in this investigation and figure 3 shows the wheel test fixture in the fixed-slip-ratio mode. Figure 4 is a close-up of the instrumented wheel test fixture in the yaw test operational mode. Also identified in figures 3 and 4 are the key components to each test operation. Vertical load was applied to the tire by means of two pneumatic cylinders and this load, together with the drag and side loads on the tire, was measured by strain gage beams in the wheel test fixture. To provide operations at fixed slip ratios, the test tire was driven through a universal coupling by interchangeable gears, which in turn were chain-driven by a driving wheel on the vehicle. Changing the slip ratio entailed merely replacing and positioning the gear at the driving end of the universal

coupling. This technique for changing slip ratio proved to be far superior to that employed in reference 1 for similar tests. For the yaw tests, the universal coupling was disconnected and, as shown in figure 4, the entire fixture rotated and clamped at the preselected yaw angle. During the fixed-slip-ratio tests on tires with elastomers C and D, and during all yaw tests, an optical pyrometer (shown in fig. 4 but removed in fig. 3) was mounted on the fixture in a position to monitor tread temperature after the tire had rotated approximately 3/8 of a revolution out of the footprint. This location of the pyrometer was necessary to avoid contaminating the sensor element. The output from the pyrometer and those from the two tire-carcass theromocouples, as collected through slip rings, were recorded on an oscillograph mounted in the vehicle driving compartment. The instrumented trailing wheel, seen in all photographs of the vehicle and identified in figures 3 and 4, provided an accurate measurement of vehicle speed and distance, and a cam-operated microswitch transmitted a signal for each test wheel revolution to the oscillograph as well as to a visual counter.

Test Technique

The testing technique involved driving the ground vehicle at a speed of 32 km/hr (20 mph) over a known distance with the test tire driven at a fixed slip ratio or freely rolling at a fixed yaw angle, depending upon the test operational mode, while the number of test wheel revolutions, the tread wear, the various tire loadings, and tire tread and carcass temperatures were monitored. Tread wear was obtained by weighing the tire and wheel assembly prior to testing and at frequent intervals during the tire test life. Since the vehicle had to be stopped and the tire and wheel assembly removed for weighing, a number of passes over a known distance were made on each surface between weighings. In general, the pass lengths were set at 305 m (1000 ft), but at the high slip ratios and the large yaw angles, where the tire wear rates were high, these lengths were necessarily reduced to, in some cases, as low as 152 m (500 ft) and the tire was weighed following each pass. At other conditions where the tread wear was slight, numerous passes were made between weighings. Several free-rolling tests were also conducted on unyawed tires at distances up to 5 km (3.1 miles) to better understand the temperature buildup in the tire carcass.

During a typical test run, either at one slip ratio or at one yaw angle, the tire was first lowered to the surface and loaded to 17.8 kN (4000 lb) while the vehicle remained stationary. The vehicle was then driven at 32 km/hr (20 mph) over the fixed distance, with the acceleration and deceleration phases as brief as possible. During the pass an oscillograph recorded the vehicle speed and distance, the test wheel revolutions, the outputs from the load beams, and, when available, the response of the two thermocouples and the optical pyrometer. Figure 5 is a reproduction of a typical oscillograph record taken during a test at a fixed slip ratio and figure 6 is typical of those taken during yaw tests of a freely rolling tire. At the conclusion of the pass, the vertical load on the tire was removed, the tire was raised from the surface, and the vehicle was realined for another pass. If a tire-wear data point was desired the tire and wheel assembly was removed and weighed at this time and then reinstalled for additional passes. Testing of a tire was concluded when most of the tread rubber had been removed. Because of the limited number of

available tires, each tire in the yaw tests was used to obtain data at two angles, and in the fixed-slip-ratio tests a tire was run at two slip ratios whenever possible.

Before and after each discrete fixed-slip-ratio test, the driving gear was disengaged and the test tire, while fully loaded, was driven over the pass length in the free-rolling or unbraked state and the number of wheel revolutions recorded. A knowledge of the braked and unbraked wheel revolutions was necessary to define the test slip ratio of the braked tire. Similarly, to obtain an equivalent braking slip ratio during the yaw tests, the tire was freely rolled at zero yaw angle prior to and following each yaw test.

RESULTS AND DISCUSSION

General

Data from the fixed slip-ratio tests included a revolution count of the freely rolling and gear-driven test wheel over the pass distance, tire weights at various distance intervals, and time histories of the vertical and drag tire loadings plus the output from the various temperature sensors, when available. These data defined the test slip ratio, the tire-tread wear rate, the drag-force friction coefficient, the approximate tread surface temperature, and the temperature of the tire carcass beneath the tread in the shoulder area. The test slip ratio was computed from the relationship

$$\text{Slip ratio} = \frac{N_o - N_b}{N_o}$$

where N_o and N_b are the number of unbraked (free-rolling) and braked test wheel revolutions, respectively, over the same distance on the test surface. The tire tread wear was determined from the cumulative loss in tire weight as a function of distance. The drag-force friction coefficient was defined as the ratio of the measured drag load to the applied vertical load.

Similar data, together with the side loading on the tire, were collected during the yaw tests. This side loading (perpendicular to the wheel plane) was converted to a side-force friction coefficient by dividing it by the applied vertical load and, subsequently, when combined with the drag-force friction coefficient measured parallel to the wheel plane, was trigonometrically transformed into cornering and drag friction coefficients, perpendicular and parallel to the vehicle direction of motion, respectively. The tire loadings, revolution count, and, when available, temperatures were monitored during every pass together with the test vehicle speed and distance. Figure 5 is a typical oscillograph record of a pass with the tire operating in the fixed-slip-ratio mode and figure 6 is typical of the yawed mode. The oscillations noted in the force-gage responses of these figures are attributed to surface unevenness, to motions in the vehicle and wheel test fixture, and to the tire elastic behavior. These oscillations occurred about faired levels which were observed to reach essen-

tially constant values throughout each pass. The friction coefficients for a pass were computed by dividing the faired drag and/or side load by the faired vertical load. Figures 5 and 6 also illustrate how, during the course of a pass, the tire-tread surface temperature generally increased to some maximum level which was essentially maintained for the remainder of the constant-speed portion of the pass. This level is referred to as the maximum tread temperature in the discussions to follow. It is readily apparent from the time histories that the tire-carcass temperature continues to increase with distance traveled. Since no equilibrium or quasi-static carcass temperature is reached during a pass, the actual measured temperatures from start to completion of each pass are presented. Temperature data from just one thermocouple are presented since only slight differences were ever noted between the temperature levels of the two transducers.

Fixed-Slip-Ratio Tests

Data which typify the results from tires operating at fixed slip ratios are presented in figure 7 for three slip ratios, where the tire wear, steady-state drag-force friction coefficient, maximum tread temperature, and carcass temperature are plotted as a function of distance traveled. These particular data are for tires with elastomer C in their tread and the testing was performed on a smooth asphalt surface. Tire wear was obtained from weighings at distance intervals commensurate with the wear rate; hence, the number of passes between weighings and the actual pass lengths decreased with increasing slip ratio. The friction coefficient as well as tread and carcass temperatures were obtained from the oscillograph records during every pass, and values of the friction coefficient and the maximum tire-tread temperatures are plotted at distances which represent the midpoint of each pass (fig. 7). The actual carcass temperatures are plotted as measured during each pass since no equilibrium value was reached. The data of figure 7 illustrate the linear relationship between tire wear and the traversed distance, and also show that over a given distance the wear increases with increasing slip ratio. The nonlinearity noted at a slip ratio of 0.396 can be explained by tread chunking which was observed with that particular combination of tire, surface, and slip ratio.

Figure 7 also shows that, for the slip ratios considered, the drag-force friction coefficient increases with increasing slip ratio. However, it is shown later that the friction level at a slip ratio of 0.396 is slightly less than the maximum which was developed at a somewhat lower slip ratio. Also, the friction coefficient remains essentially constant with distance during operations at a given slip ratio, although it appears to increase slightly, particularly at the higher slip ratios. Both the magnitude of the maximum tread temperature and the rate of temperature rise in the tire carcass increase with increasing slip ratio (fig. 7).

The following paragraphs examine in some detail the effects of slip ratio on tread wear, drag-force friction coefficient, and maximum tire-tread surface temperature for the four tire-tread elastomers operating on the three test surfaces (figs. 8 to 11). Also included is a discussion of the results from separate studies to examine the temperature buildup in the tire carcass during fixed-slip-ratio and free-rolling operations (figs. 12 and 13).

Tread wear.- Wear data from tires equipped with treads made from the four elastomers operating on the three test surfaces are summarized in figure 8. This figure relates the tire-wear rate to slip ratio, where the rate is defined by the slope of the wear/distance curves such as those presented on the bottom of figure 7. The data from all three surfaces clearly indicate that the 100-percent natural rubber tread (elastomer A) is the least wear resistant of the four elastomers and the state-of-the-art tread (elastomer B) is the most wear resistant. Treads fabricated from the two experimental elastomers had similar wear characteristics that approached those of the state-of-the-art tread. It is apparent from figure 8 that the tire-wear rate is influenced by the nature, or texture, of the surface. The lower plot of figure 10 better illustrates this surface effect. The data of figure 10 are for treads with elastomer A and are typical of all treads examined in terms of the relative difference between the wear rates on the different surfaces. Tire wear on the smooth asphalt is significantly less than that on the coarse asphalt or concrete surfaces, particularly at the high slip ratios. Wear on the latter two highly textured surfaces is quite similar. The wide difference in the wear rates associated with the two asphalt test surfaces, as noted in the data of figures 8 and 10, serves to validate the observation made in reference 1 that surface texture is a major factor in tire-tread wear.

Friction.- The variation of drag-force friction coefficient with slip ratio for the different combinations of tire-tread elastomers and surfaces is presented in figure 9. Each plotted value of friction coefficient represents the average of that measured over the life of the tread at each slip ratio. The figure shows that the developed friction is essentially independent of the elastomer since one curve appears to fair all the data gathered from each surface over the slip-ratio test range. The effect of test surface on friction can be obtained by comparing the three sets of data in figure 9 or by examining the upper plot of figure 10 which presents all the friction data collected from tires equipped with elastomer A during fixed-slip-ratio operations. As has been noted in other references (e.g., refs. 1 and 3), the friction coefficient is generally insensitive to the character of the runway surface when dry.

The magnitude of the maximum friction coefficient developed under the conditions of these tests is approximately 0.8, which is in good agreement with the value of 0.81, predicted from the empirical expression developed in reference 4 at very low ground speeds. However, when compared with the friction data of reference 1, which reports on similar tests on the same size of aircraft tire, there is a difference in the slip ratio at which the maximum friction coefficient is developed. Maximum friction in reference 1 occurred at a slip ratio of approximately 0.18, whereas in the current tests the maximum occurred at slip ratios in the 0.30 to 0.40 range. The explanation for this difference could be the lower inflation pressure (738 versus 827 kPa (107 psi versus 120 psi)) and higher ply rating (12 versus 8) of the tires in these tests.

Temperatures.- Difficulties early in the program with a variety of optical pyrometers limited measurements of the tire-tread temperatures to only tires equipped with elastomers C and D, the experimental elastomers, in the fixed-slip-ratio phase of this program. The maximum approximate tread surface temperatures reached by these tires on the three test surfaces are presented in fig-

ure 11. These temperatures are the average of those recorded during each pass over the life of the tread at a fixed slip ratio. Figure 11 shows that the tread temperature is insensitive to the elastomer and that the temperatures generated during operations on concrete are less than those generated on asphalt at the same slip ratio. Similar trends were observed in reference 1 and explained on the basis of thermal conductivity. The conductivity of asphalt is less than that of concrete; therefore, more heat is dissipated to the concrete which results in a cooler tire tread. It is interesting to note that the temperatures of figure 11 are slightly higher than the temperatures recorded at the same slip ratio in reference 1. The difference in the inflation pressures and ply ratings of the two sets of tires is again offered as an explanation.

It is readily apparent from the sample oscillograph record of figure 5 and the typical results of figure 7 that the temperature in the tire carcass, beneath the tread in the shoulder area, does not reach equilibrium during the course of a pass. Thus, it is meaningless to assign a carcass temperature value to each pass. Figure 7 does suggest however, that the rate of temperature buildup in the carcass varies with slip ratio and, as noted in the data at a slip ratio of 0.187, the rate of that buildup appears to increase with subsequent passes. Figure 12 was prepared to better illustrate these points. In this figure, the measured temperature increase per unit distance traveled is plotted as a function of slip ratio for tires equipped with elastomer C operating on the smooth asphalt surface. Each data point is identified with a number that corresponds to the pass number at each slip ratio. The data are bounded by two curves. The lower curve fairs the first-pass values and is labeled "new tread," and the upper curve fairs the last-pass values, where most or all of the tread rubber had been removed, and is labeled "worn tread." Very little tread was removed as a result of eight passes at the lowest slip ratio identified in this figure. Figure 12 shows that the rate of temperature buildup in the carcass increases with increasing slip ratio, and further, that the rate increases with decreasing tread depth. These increases are attributed to greater carcass flexing which can be expected to occur at higher slip ratios and to the transfer of heat into the carcass from the much hotter tread surface. Transfer of heat is perhaps an explanation for the increased rates during subsequent passes at one slip ratio since the distance from the embedded thermocouple to the hot tread surface decreases with each pass.

In view of the limited available experimental data which describe the temperatures generated beneath the tread of an aircraft tire, several additional tests were conducted specifically to give a better understanding of tire-carcass temperatures. The results from these tests, all performed with a free-rolling unyawed tire, are presented in figure 13. Figure 13(a) shows the effect of test speed on carcass temperature where tires equipped with thermocouples were loaded to 17.8 kN (4000 lb) and exposed to three passes approximately 2.5 km (8200 ft) long down an active runway at three test speeds. The vehicle speed during one test was increased on each subsequent pass with a relatively long pause for runway availability between passes. The speed for the other test was 84 km/hr (52 mph) for the first pass, 32 km/hr (20 mph) for the second, and 64 km/hr (40 mph) for the third with somewhat shorter pauses between them. It appears that at the conclusion of both tests the tires were approaching an equilibrium temperature slightly greater than 80° C. Figure 13(a) shows that the rate of carcass temperature rise appears to be a function of test speed, tending to

increase with speed, and the temperature differential with respect to the equilibrium temperature. More precisely, the colder the tire at the onset of the test, the greater the rate of temperature rise. In an attempt to validate the existence of a possible equilibrium temperature under the loading conditions of these tests, one of the tires was subjected to two passes over a 5-km (3.1 miles) highway route at a constant speed of 32 km/hr (20 mph). The carcass temperature recorded during those passes is plotted as a function of distance in figure 13(b) and, as in the earlier tests, it appears as though the temperature approaches 83° C as an asymptote which suggests that value as an equilibrium temperature under those test conditions.

Figure 13(c) shows the effect of underinflation on carcass temperature. Data are presented for similar passes with the tire at its normal test inflation pressure of 738 kPa (107 psi) and at a pressure of 641 kPa (93 psi). As would be expected, because of the increased carcass flexing under the same vertical load, the underinflated tire experienced higher temperatures and in time would no doubt reach a somewhat higher equilibrium temperature.

The findings from these temperature studies are in agreement with those from similar studies conducted on automotive tires. (See refs. 5 to 8 for examples.)

Yaw Tests

Figure 14 presents typical results from the yaw tests for tires retreaded with elastomer C and operated on smooth asphalt. Tire wear, side-force friction coefficient, maximum tread temperature, and carcass temperature are plotted as a function of distance traveled at yaw angles ψ of 8°, 12°, and 20°. As in the fixed-slip-ratio tests, tire wear was obtained from weighings at distance intervals commensurate with the wear rate; hence the number of passes between weighings and the actual pass lengths decreased with increasing yaw angle where the wear was more pronounced. For the data of figure 14, weighings occurred after every pass, but the pass length decreased from 305 m (1000 ft), at $\psi = 8°$ and 12°, to 152 m (500 ft) at $\psi = 20°$. The friction and temperature data were taken from oscillograph records during every pass and values of the side-force friction coefficient and maximum tire-tread temperature are plotted in the figure at distances which represent the midpoint of each pass. Again, no equilibrium carcass temperature was reached; hence the actual temperatures are plotted in the figure. The data of the figure exemplify the linear variation of tire wear with distance traveled and show that over a given distance the wear increases with increasing yaw angle. The side-force friction coefficient, which is based upon the force developed perpendicular to the wheel plane, increases, as expected, with increasing yaw angle and appears to be relatively constant throughout the test distance, although a slight increase can be observed at the highest yaw angle presented. Figure 14 also shows that the maximum tire-tread temperature increases with yaw angle but that the rate of temperature buildup in the carcass (at least, at the site of the installed thermocouples) appears to decrease with yaw.

The detailed effects of yaw angle on tire wear, cornering, and drag friction coefficients and the various tire temperatures are discussed in the following paragraphs.

Tread wear.- The wear data from the treads of the freely rolling tires in the yaw tests are summarized in figure 15 where the wear rate is plotted as a function of the yaw angle. The different symbols identify the four tread elastomers examined. As was the case in the fixed-slip-ratio tests, the current state-of-the-art tread, elastomer B, is the most resistant to wear and the natural rubber tread, elastomer A, is the least wear resistant. The wear rate of the two experimental elastomers, although better than natural rubber, did not demonstrate the significant improvement noted in the fixed-slip-ratio tests (fig. 8). The data of figure 15 depict clearly the increase in tire-wear rate with increasing yaw angle, despite a certain amount of scatter.

Friction.- The side-force friction coefficient of figure 14 is the ratio of the side load on the tire, perpendicular to the wheel plane, to the vertical load and, as observed in the figure, can reach levels at least as high as 0.75. However, the drag load parallel to the wheel plane is observed to be quite small in the time history of figure 6 and, on the basis of these and other tests, is assumed equal in magnitude to the tire rolling resistance regardless of yaw angle within the range of the tests reported herein. These tire loadings were trigonometrically transformed to the tire cornering force, perpendicular to the vehicle motion, and drag force, parallel to the vehicle motion. Both are presented in coefficient form in figure 16. As was observed in the fixed-slip-ratio tests, the friction coefficients appear to be independent of the tread elastomer since each cornering friction coefficient suggests a peak value of approximately 0.65 near a yaw angle of 25°. The drag-force friction coefficient, as expected, shows a gradual increase with yaw angle. By definition, the drag-force friction coefficient will reach a maximum value at a yaw angle of 90° where the cornering-force friction coefficient would reduce to zero.

Temperatures.- Figure 17 presents the maximum approximate tread surface temperatures measured by the optical pyrometer as tires with elastomers B, C, and D were subjected to the range of test yaw angles. The data suggest that the tread temperature is independent of the elastomer as was observed in the fixed-slip-ratio tests. The temperature is shown to increase with increasing yaw angle which would be expected since the tire experiences a greater scrubbing action at the higher yaw angles.

An examination of the carcass temperatures presented in figure 14 suggests that the rate of temperature buildup in the carcass is reduced when the yaw angle is increased. This reduction is attributed to the physical location of the embedded thermocouples. In the test described by figure 14, the shoulder area housing the thermocouples was not rolled into the footprint when the tire was yawed; thus the rate of temperature buildup tended to decrease as the yaw angle was increased. One series of tests was conducted where, during yaw, the instrumented shoulder of the tire was rolled into the footprint. For these latter tests, the rate of temperature rise increased rapidly with increasing yaw angle. In either set of tests, no attempt was made to establish an equilibrium temperature at any yaw angle.

Braking and Cornering Relationships

The purpose of this section is to attempt to relate tread wear, friction, and temperature data between an unbraked, yawed tire and a braked, unyawed tire. To effect this relationship, the assumption is made that these tire characteristics are the direct result of the relative slip velocity between the tire and the pavement. Thus, it is assumed that if the resultant slip velocity is the same, whether stemming from braking or yawing a tire, the magnitude of these tire characteristics would be the same.

For a braked, unyawed tire the lateral slip velocity is zero and hence the resultant slip velocity $V_{r,b}$ equals the slip velocity in the fore-and-aft direction. The simple relationship

$$V_{r,b} = V_g R_s \tag{1}$$

applies where V_g is the vehicle ground speed and R_s is the braking slip ratio.

For an unbraked, yawed tire the lateral slip velocity is $V_t \sin \psi$, where V_t is the tire circumferential velocity and ψ is the yaw angle. The slip velocity in the fore-and-aft direction for the yawed tire is the difference $V_g - V_t \cos \psi$. For small yaw angles, V_t can be approximated by V_g; thus, the lateral slip velocity becomes $V_g \sin \psi$ and the fore-and-aft slip velocity becomes $V_g(1 - \cos \psi)$. Data collected during the course of the yaw tests to aid in validating the fore-and-aft portion of this approximation are reproduced in figure 18. This figure presents, as a function of yaw angle, the equivalent fore-and-aft slip ratio as determined experimentally from the relationship

$$\text{Equivalent fore-and-aft } R_s = \frac{N_o - N_\psi}{N_o} \tag{2}$$

where N_o is the number of revolutions of the unbraked and unyawed test wheel over a specified distance and N_ψ is the number of revolutions of the unbraked, yawed tire over the same distance. These faired data are compared with the curve described by $(1 - \cos \psi)$ which, for small angles, corresponds to the equivalent fore-and-aft slip ratio for the yaw tests. The figure suggests that the small-angle assumption is a good one. Thus, the resultant slip velocity $V_{r,\psi}$, which is the vectorial sum of the lateral and fore-and-aft slip velocities, simply becomes

$$V_{r,\psi} = V_g \sqrt{2(1 - \cos \psi)} \tag{3}$$

A comparison of equations (1) and (3) suggests that the tread characteristics of tires operating in the two modes can be compared on the basis of slip ratio where, in the yawed case, an equivalent slip ratio is computed for each yaw angle by the expression

$$\text{Equivalent resultant} \quad R_S = \sqrt{2(1 - \cos \psi)} \tag{4}$$

Figures 19, 20, and 21 compare the tire wear rate, friction coefficient, and tread surface temperature, respectively, of the pure braking operational mode with those of the pure yawing operational mode. The comparison is made on the basis of resultant slip ratio. For the braking case in figure 19, the faired tire-wear-rate curves of figure 8 for smooth asphalt are replotted. For the yawing case, the faired data of figure 15 are repeated with the yaw angle converted to the equivalent slip ratio as defined by equation (4). The figure shows that at the same equivalent slip ratio, or at the same resultant slip velocity, the tread wear in braking and cornering are similar with the exception of elastomer D.

The friction coefficients of figure 20 for the braking mode are represented by the fairing of the smooth asphalt data of figure 9. Those for the unbraked yawing mode are the vector sum of the cornering and drag coefficients of figure 16 plotted as a function of the equivalent slip ratio. The maximum friction defined by the yawing mode at the highest test yaw angle, which corresponds to an equivalent slip ratio of 0.42, is shown in the figure to approach the maximum friction level defined by the braking mode. The difference at the low slip ratios is due perhaps to differences between the lateral and fore-and-aft elastic behavior of the tire. Aircraft tires are stiffer in the fore-and-aft (braking) direction than in the lateral direction. Unpublished data on tires of similar size show fore-and-aft spring constants which typically double the lateral spring constants for the same loading conditions. The softer tire carcass would tend to reduce the relative slippage between the tire and the pavement, thus resulting in a lower friction level. This corresponding lower effective slip ratio in yawing compared with that in braking may also explain the lower wear rates of figure 19 and the lower tire-tread surface temperatures noted in figure 21.

CONCLUSIONS

An experimental investigation was conducted to evaluate the wear, friction, and temperature characteristics of aircraft tire treads fabricated from different elastomers. Braking and cornering tests were performed on size 22 × 5.5, type VII aircraft tires retreaded with currently employed and experimental elastomers. The braking tests consisted of gearing the tire to a driving wheel of a ground vehicle to provide operations at fixed slip ratios on dry surfaces of smooth and coarse asphalt and concrete. The cornering tests involved freely rolling the tire at fixed yaw angles of 0° to 24° on the dry smooth asphalt surface. The results of this investigation suggest the following conclusions:

1. Cumulative tire wear (tread rubber removed) varies linearly with distance traveled at all slip ratios and yaw angles, and the wear rate (mass removed per unit distance) increases with increasing slip ratio during braking and increasing yaw angle during cornering. Of the four tread elastomers investigated, 100-percent natural rubber was the least wear resistant and the state-of-the-art elastomer, comprised of a 75/25 polyblend of cis-polyisoprene and cis-polybutadiene, proved most resistant to wear. As observed in earlier tests, tread wear is highly influenced by the character of the runway surface.

2. The magnitude of the friction coefficient developed during braking and yawing is independent of the tread elastomer. The drag-force friction coefficients measured from the fixed-slip-ratio tests are in good agreement with those observed in other investigations in that they are insensitive to the character of the runway surface when dry.

3. Tread surface temperature increases with increasing slip ratio and increasing yaw angle and is independent of the elastomer. The temperatures generated during braking operations on concrete are less than those generated on asphalt.

4. Tire carcass temperature beneath the tread in the shoulder area never reached an equilibrium value over the short test lengths during either the braking or cornering operations. The rate of temperature buildup did increase with increasing slip ratio in the braking tests and is attributed to tire flexing which becomes more pronounced as slip ratios are increased. During free-rolling unyawed tests this temperature appears to reach an equilibrium value at a rate dependent upon the test speed and the temperature differential. An underinflated tire generates higher carcass temperatures due to the increased tire flexure.

5. A comparison of tire tread data obtained during the cornering tests with those from the braking tests on the basis of equivalent slip velocities suggests that the amount of tread wear is comparable but friction and surface temperatures are greater during braking operations. The difference is attributed to the tire being softer in the lateral direction which would tend to reduce the relative slippage between the tire and the pavement and therefore provide a lower effective slip ratio in cornering.

Langley Research Center
National Aeronautics and Space Administration
Hampton, VA 23665
November 9, 1979

REFERENCES

1. McCarty, John Locke: Wear and Related Characteristics of an Aircraft Tire During Braking. NASA TN D-6963, 1972.

2. Yager, Thomas J.; McCarty, John L.; Riccitiello, S. R.; and Golub, M. A.: Developments in New Aircraft Tire Tread Materials. Aircraft Safety and Operating Problems, NASA SP-416, 1976, pp. 247-256.

3. Leland, Trafford J. W.; Yager, Thomas J.; and Joyner, Upshur T.: Effects of Pavement Texture on Wet-Runway Braking Performance. NASA TN D-4323, 1968.

4. Smiley, Robert F.; and Horne, Walter B.: Mechanical Properties of Pneumatic Tires With Special Reference to Modern Aircraft Tires. NASA TR R-64, 1960.

5. Conant, F. S.: Tire Temperatures. Rubber Chem. Technol., vol. 44, no. 2, 1971, pp. 397-439.

6. Nybakken, G. H.; Collart, D. Y.; Staples, R. J.; Lackey, J. I.; Clark, S. K.; and Dodge, R. N.: Preliminary Measurements on Heat Balance in Pneumatic Tires. NASA CR-121239, 1973.

7. Clark, S. K.: Temperature Rise-Times in Pneumatic Tires. DOT/TST-75-144, U.S. Dep. Trans., Dec. 1975. (Available from NTIS as PB 266 652/7.)

8. Clark, S. K.; and Loo, M.: Temperature Effects on Rolling Resistance of Pneumatic Tires. DOT-TST-76-93, U.S. Dep. Trans., Apr. 1976. (Available from NTIS as PB 263 622/3.)

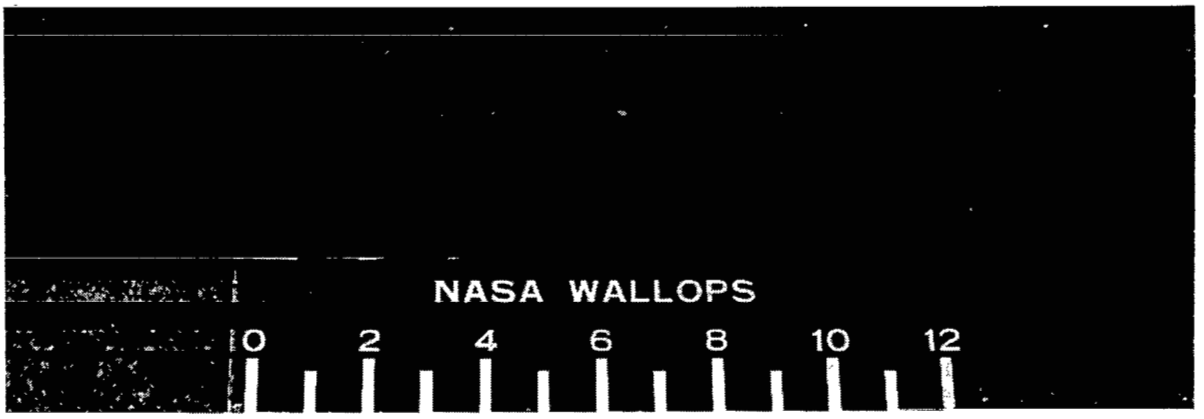

(a) Coarse asphalt.

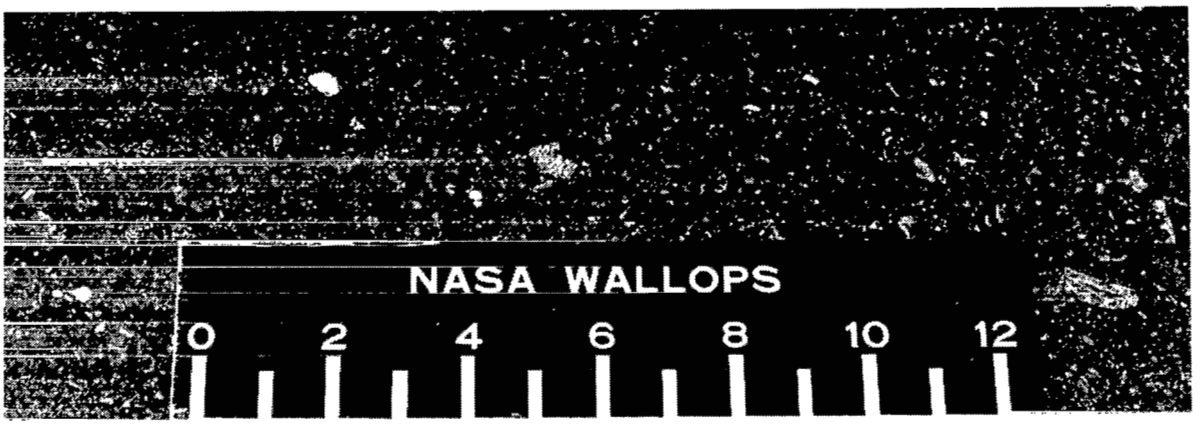

(b) Smooth asphalt.

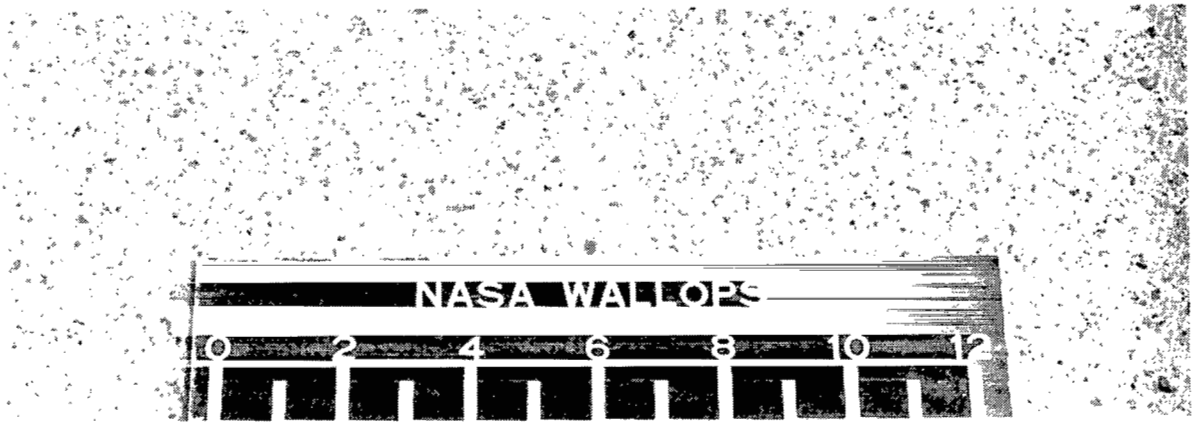

(c) Concrete.

L-79-316

Figure 1.- Close-up photographs of test surfaces. Scale in inches (1 in. = 2.54 cm).

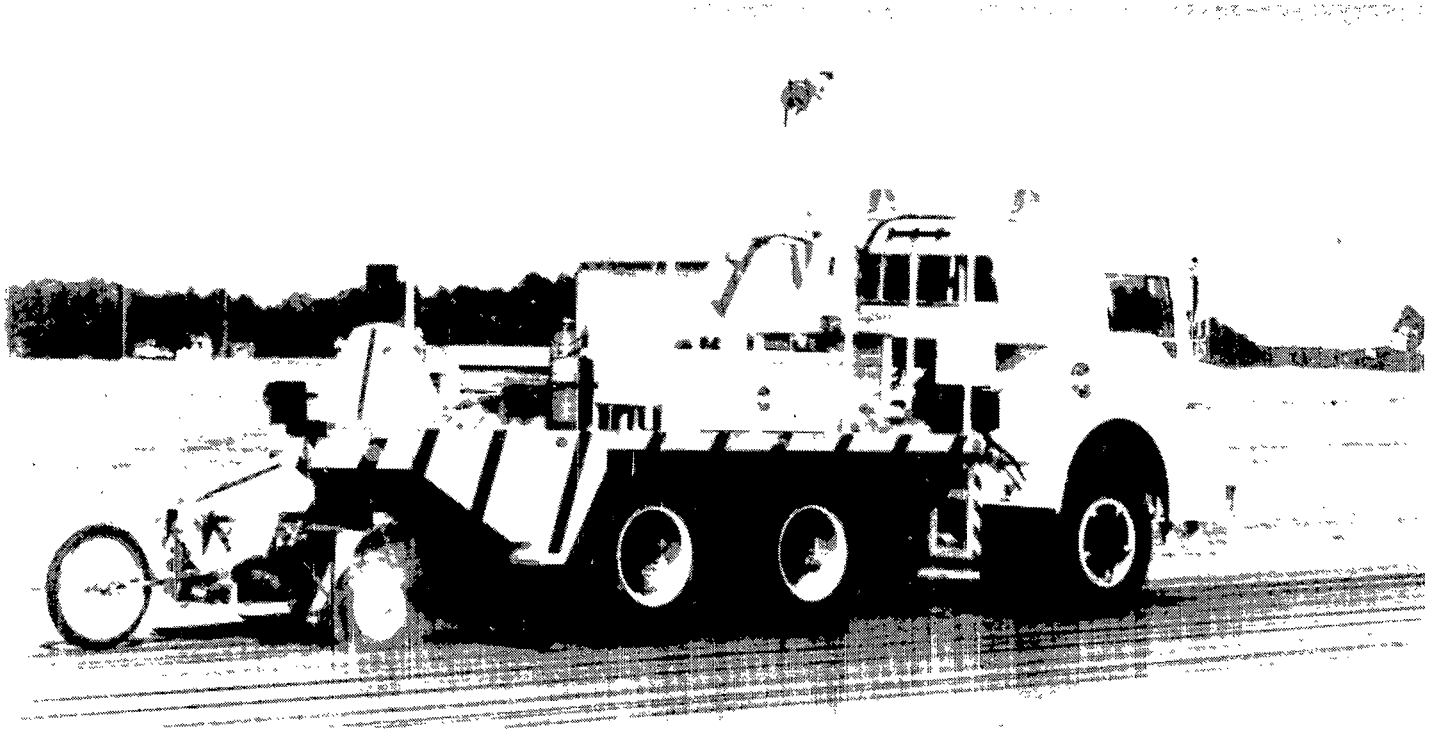

L-79-317

Figure 2.- Ground test vehicle.

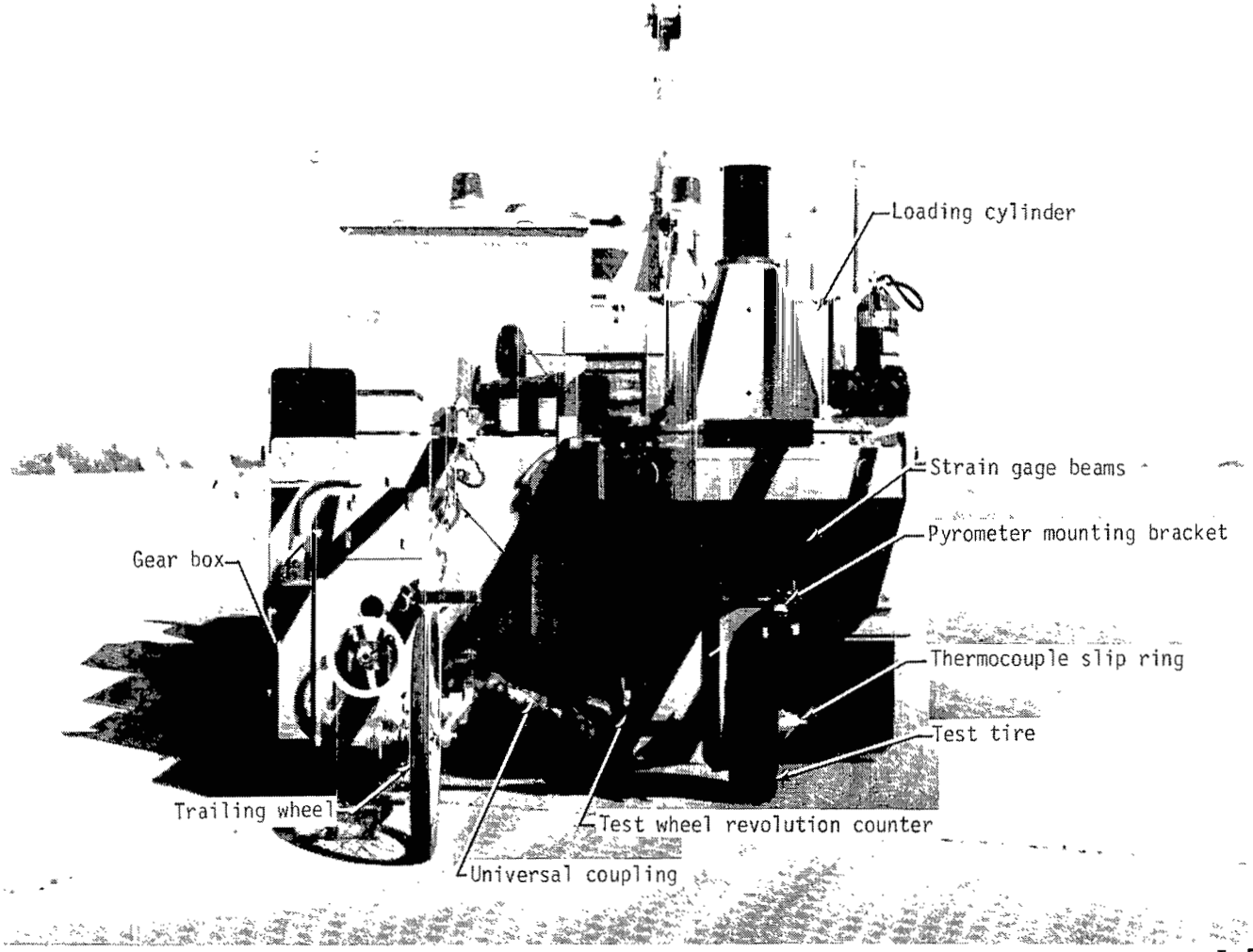

L-79-318

Figure 3.- Wheel test fixture in fixed-slip-ratio mode showing major components.

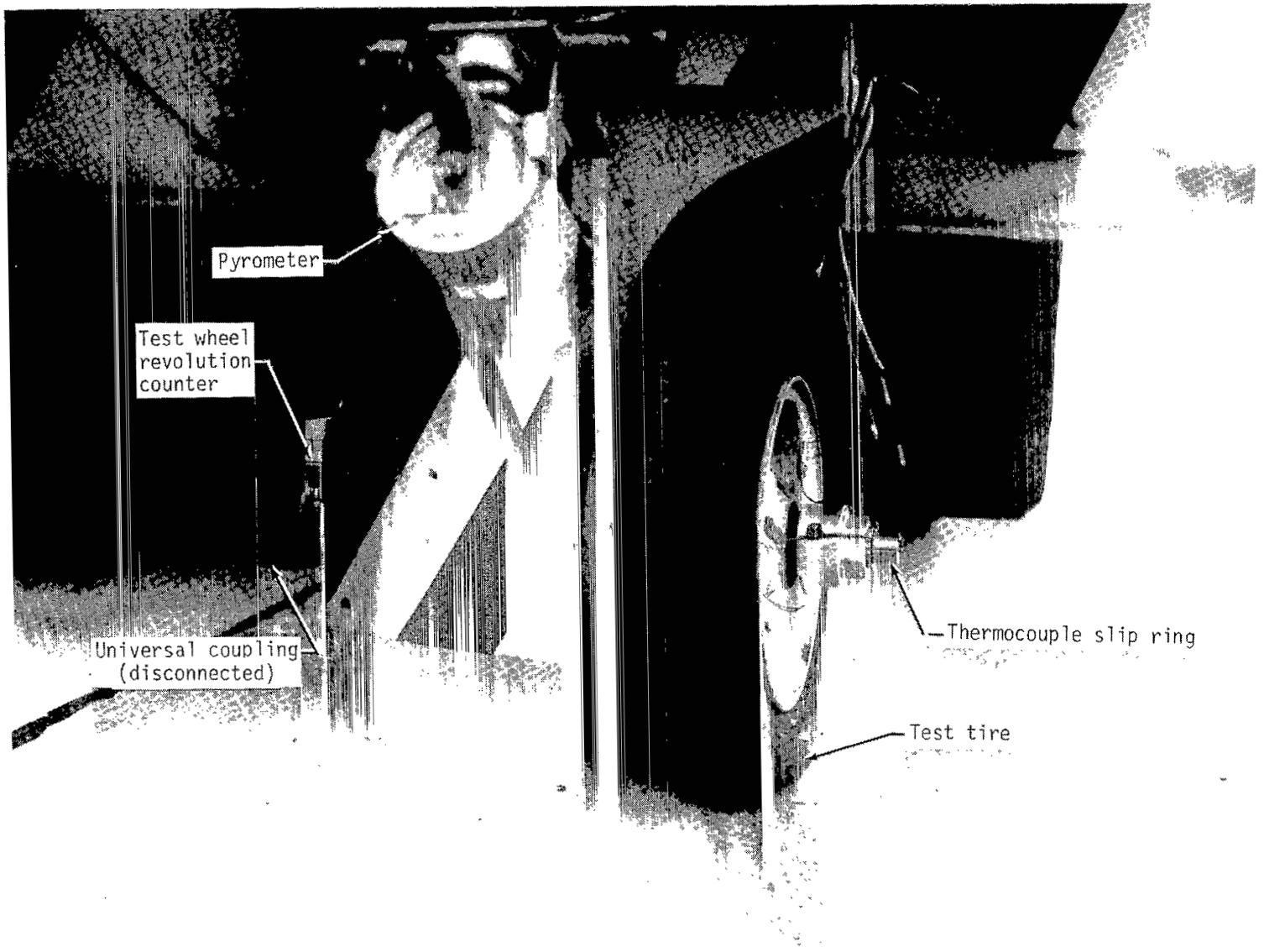

L-78-2220.1

Figure 4.- Close-up of wheel test fixture in yaw operational mode showing major components.

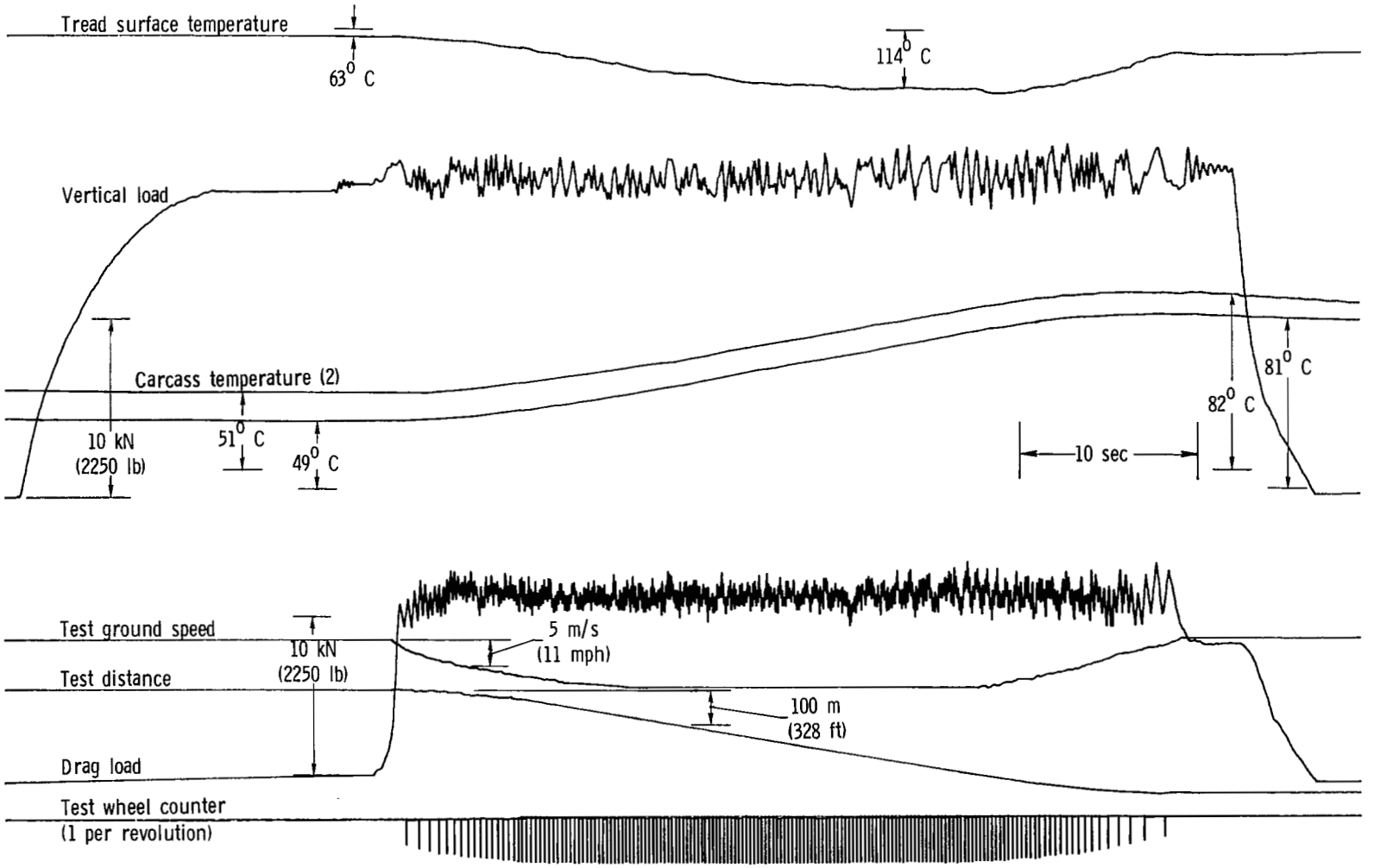

Figure 5.- Reproduction of typical oscillograph record showing instrumentation response during fixed-slip-ratio operations. Slip ratio = 0.137; concrete runway surface.

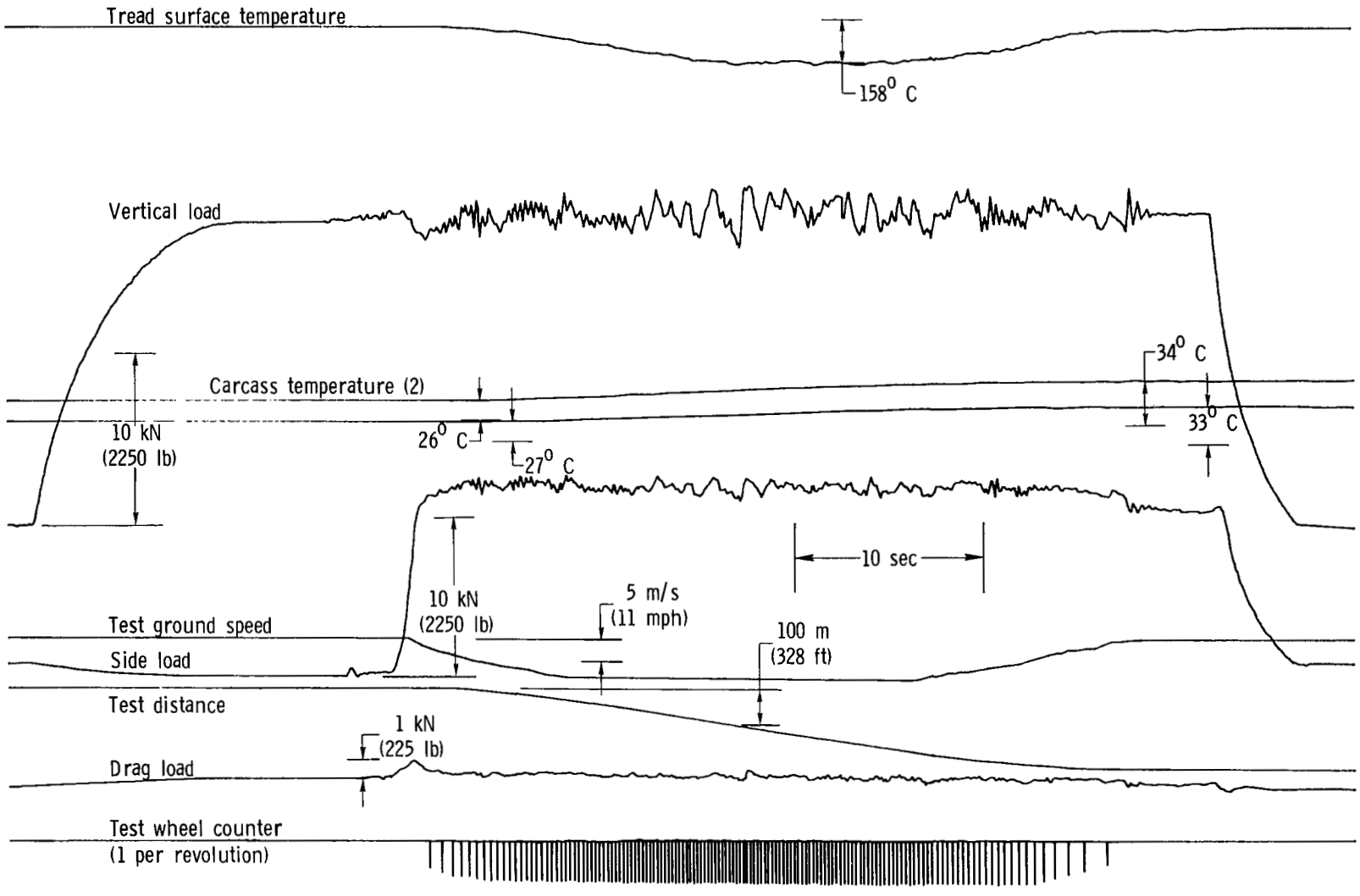

Figure 6.- Reproduction of typical oscillograph record showing instrumentation response during yaw operations of freely rolling tires. Yaw angle = 16°; smooth asphalt runway surface.

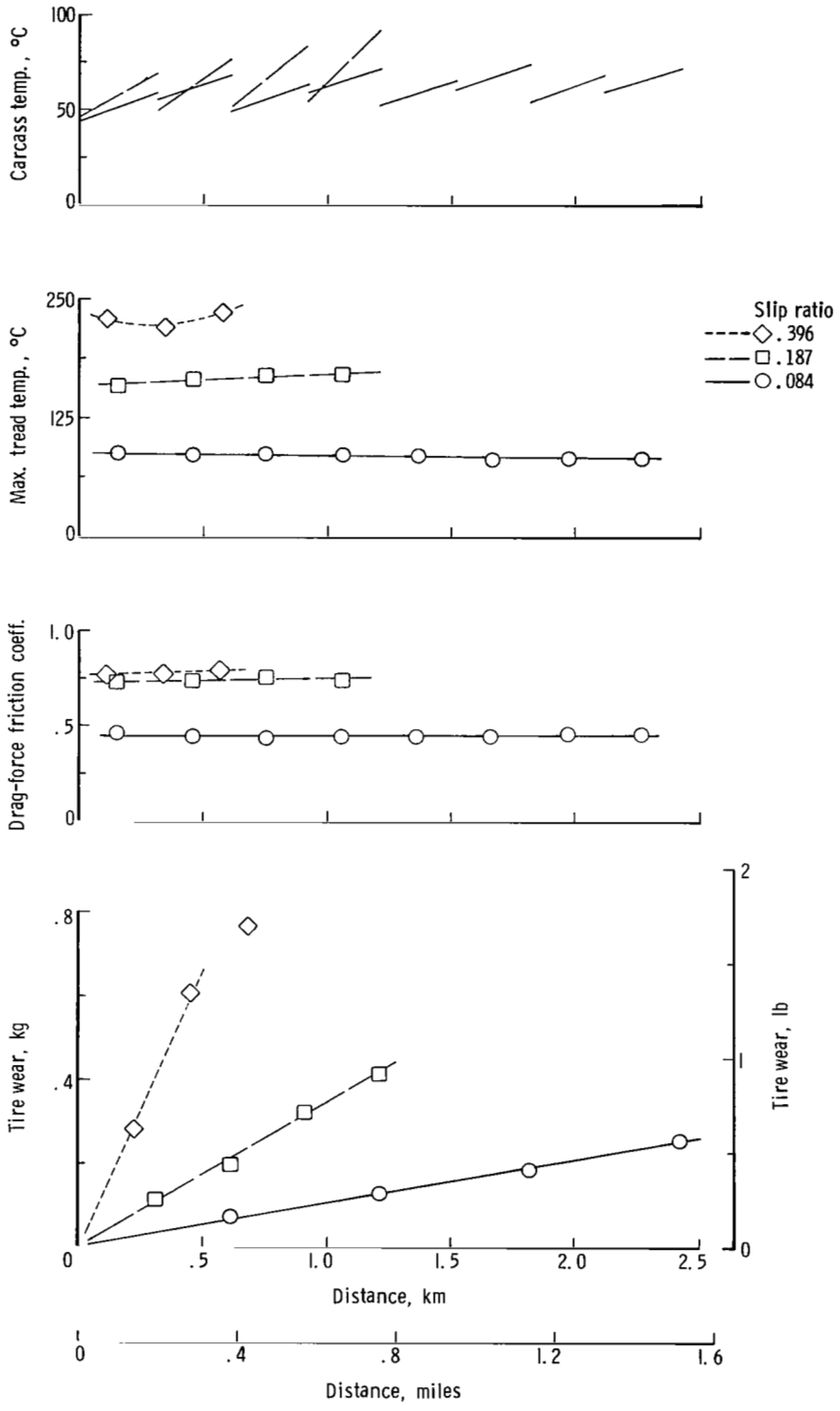

Figure 7.- Typical test results from tires operating at fixed slip ratios. Tire treads with elastomer C on smooth asphalt runway surface.

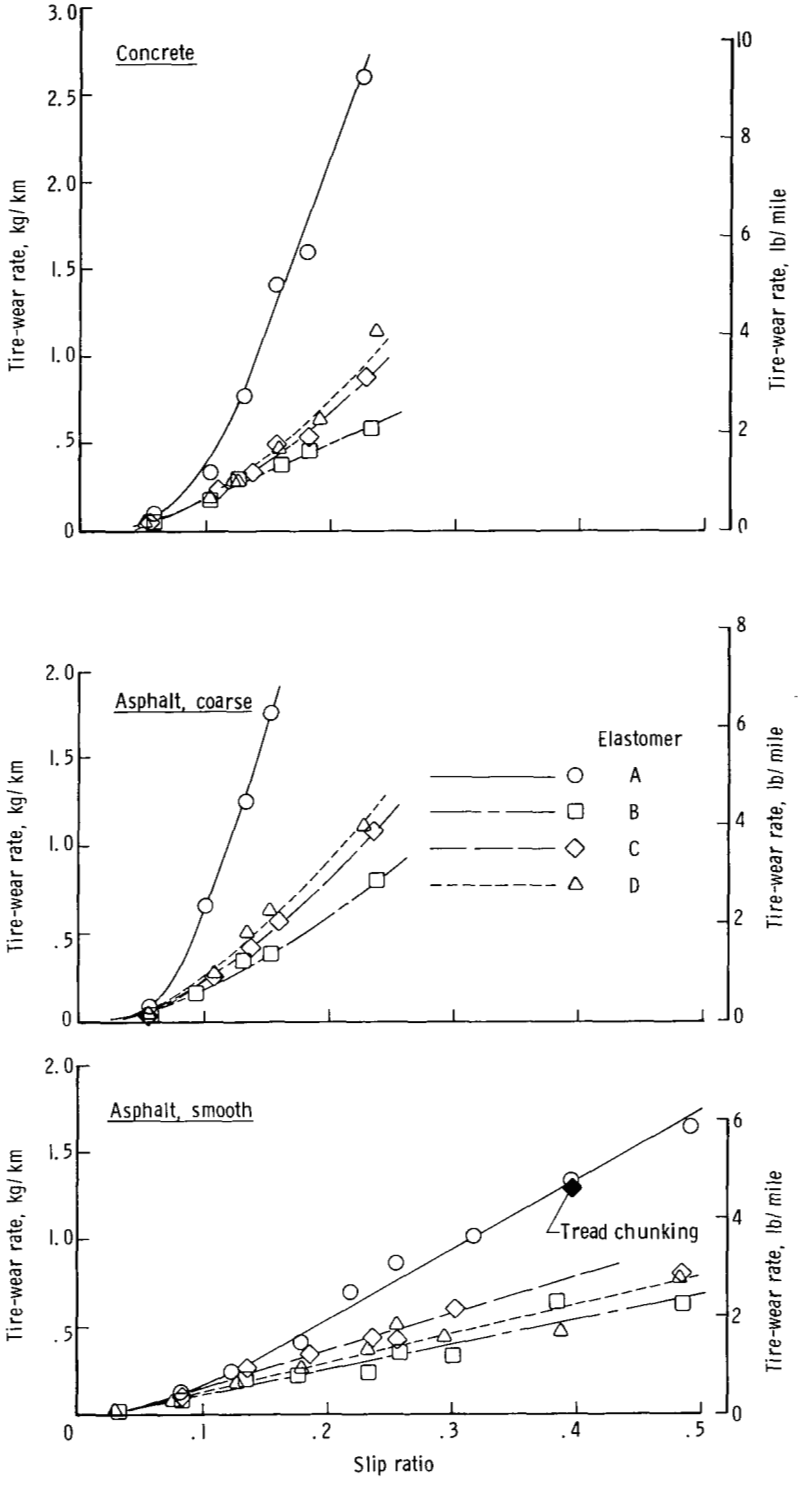

Figure 8.- Variation of tire-wear rate with slip ratio during fixed-slip-ratio operations with test tread elastomers on three runway surfaces.

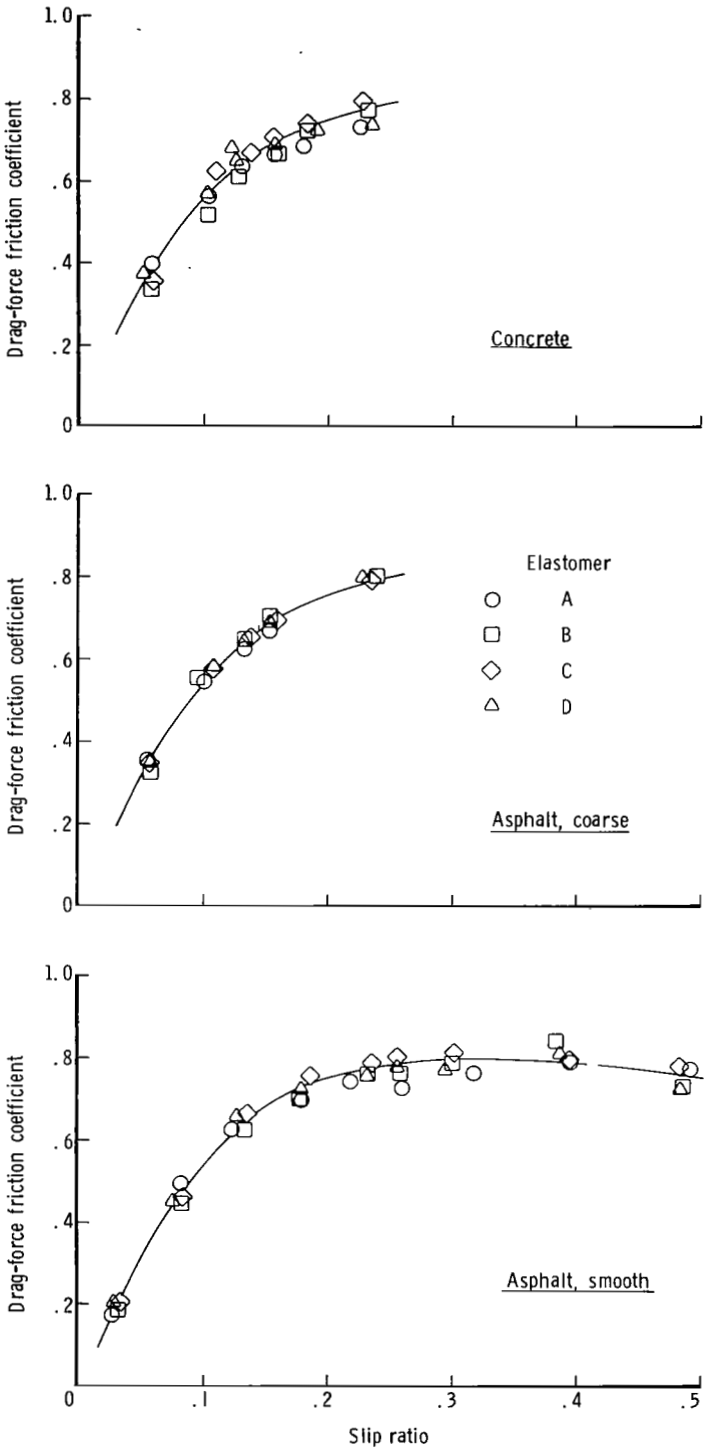

Figure 9.- Variation of drag-force friction coefficient with slip ratio during fixed-slip-ratio operations with test tread elastomers on three runway surfaces.

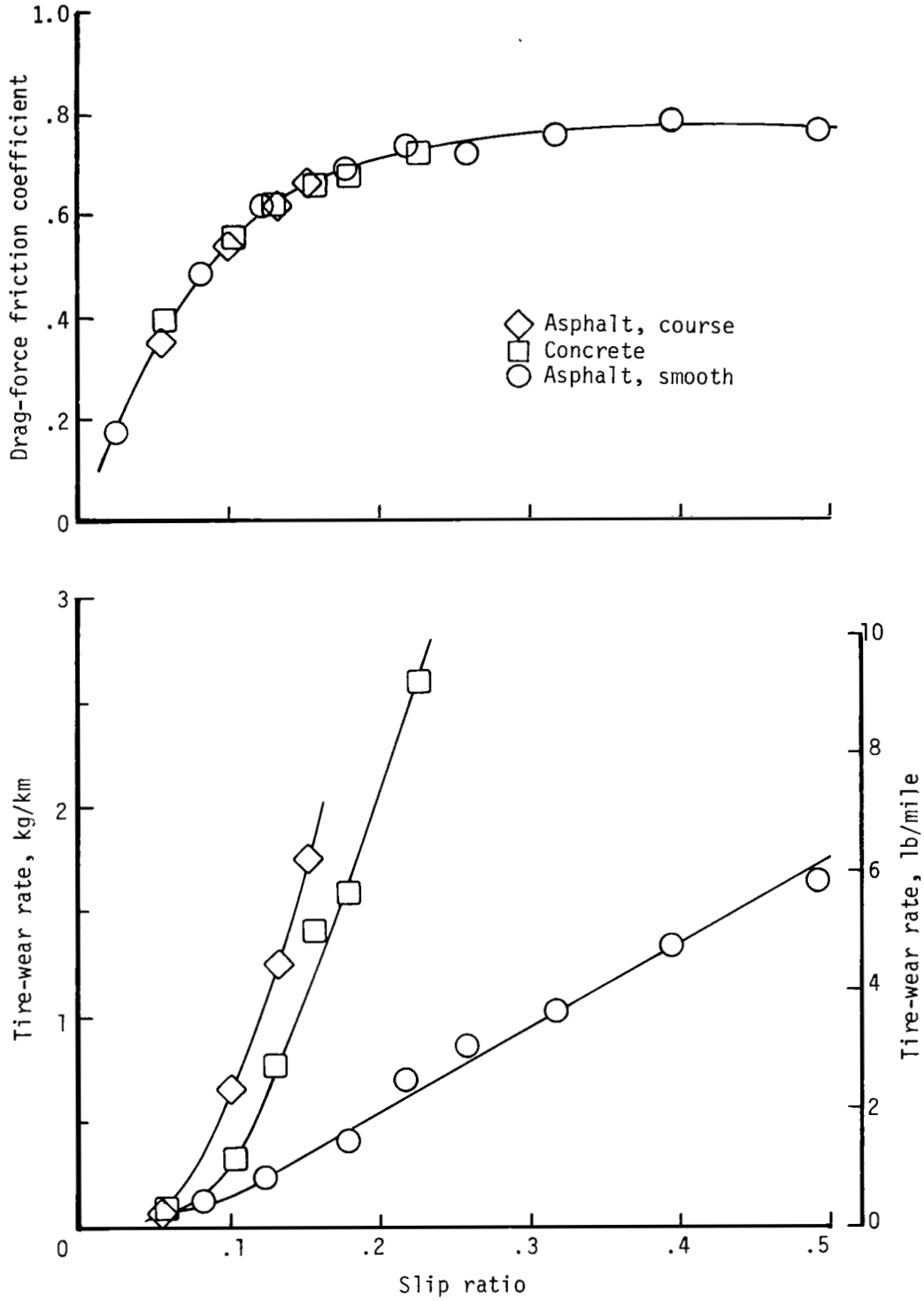

Figure 10.- Effect of runway surface on tire-tread wear rate and drag-force friction coefficient developed during fixed-slip-ratio operations. Elastomer A.

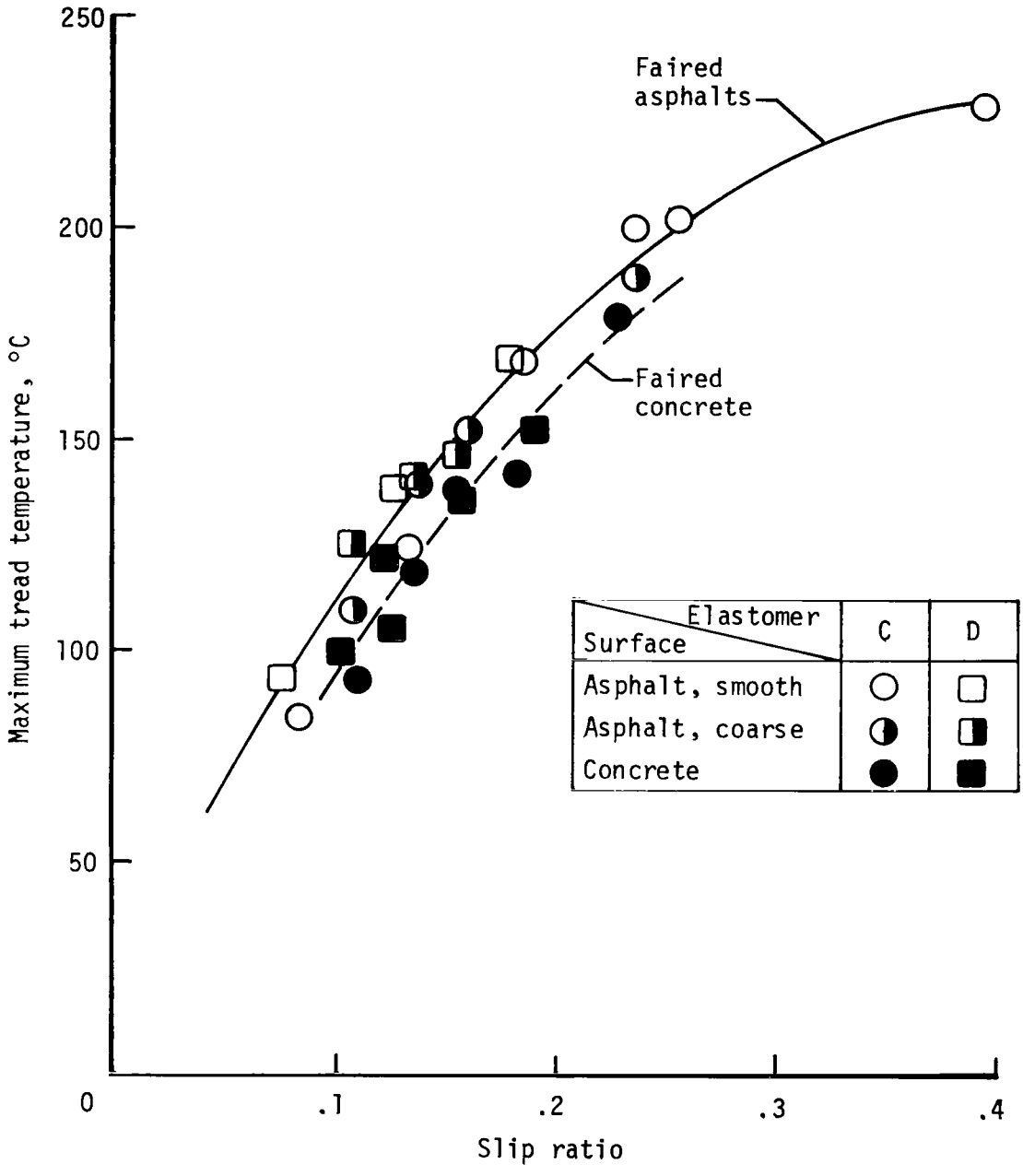

Figure 11.- Maximum approximate tire-tread surface temperatures measured during fixed-slip-ratio operations on test surfaces.

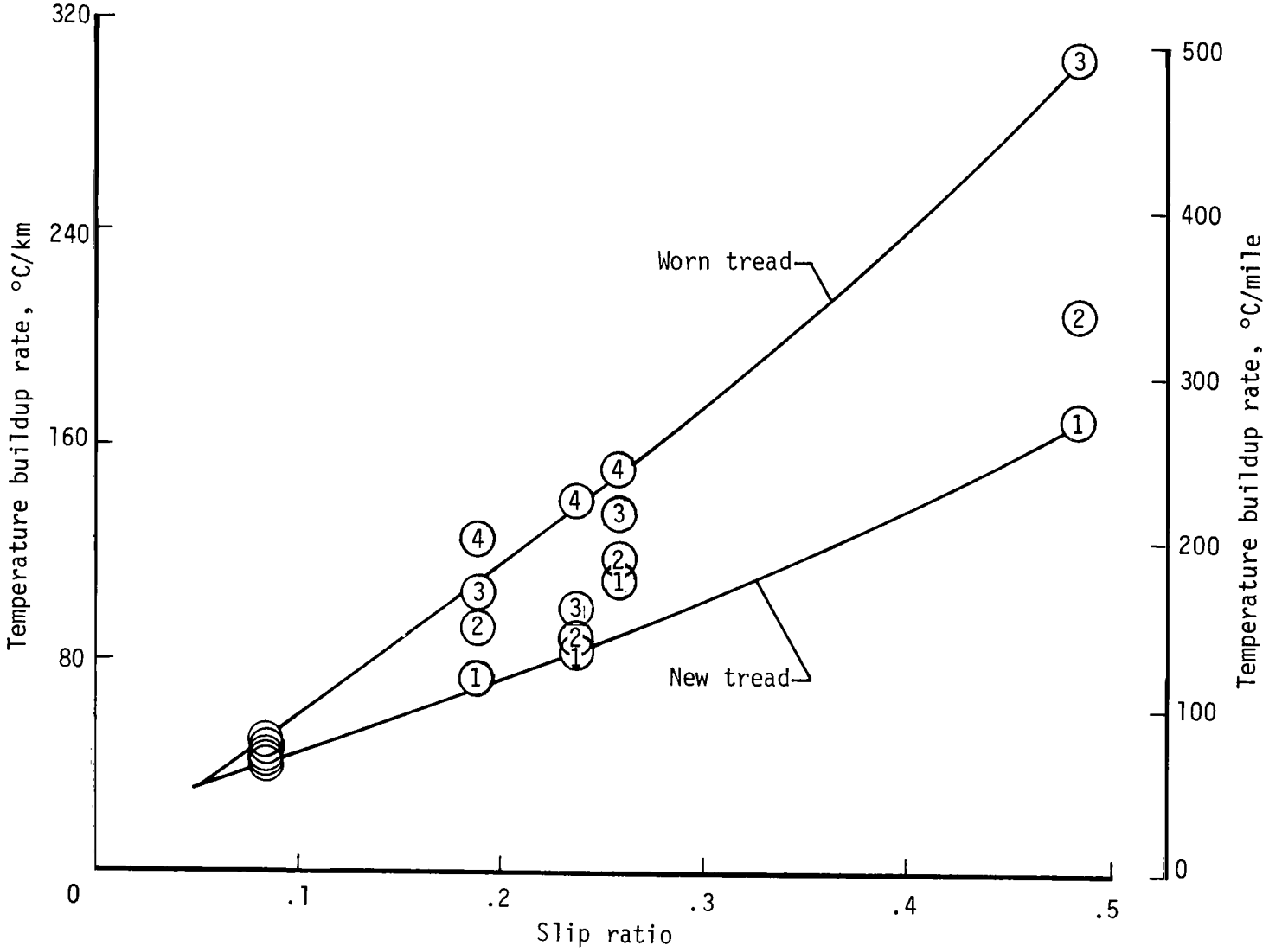

Figure 12.- Effect of slip ratio on tire-carcass temperature buildup rate. Elastomer C on smooth asphalt runway surface. Numbers in symbols refer to pass sequence at each slip ratio.

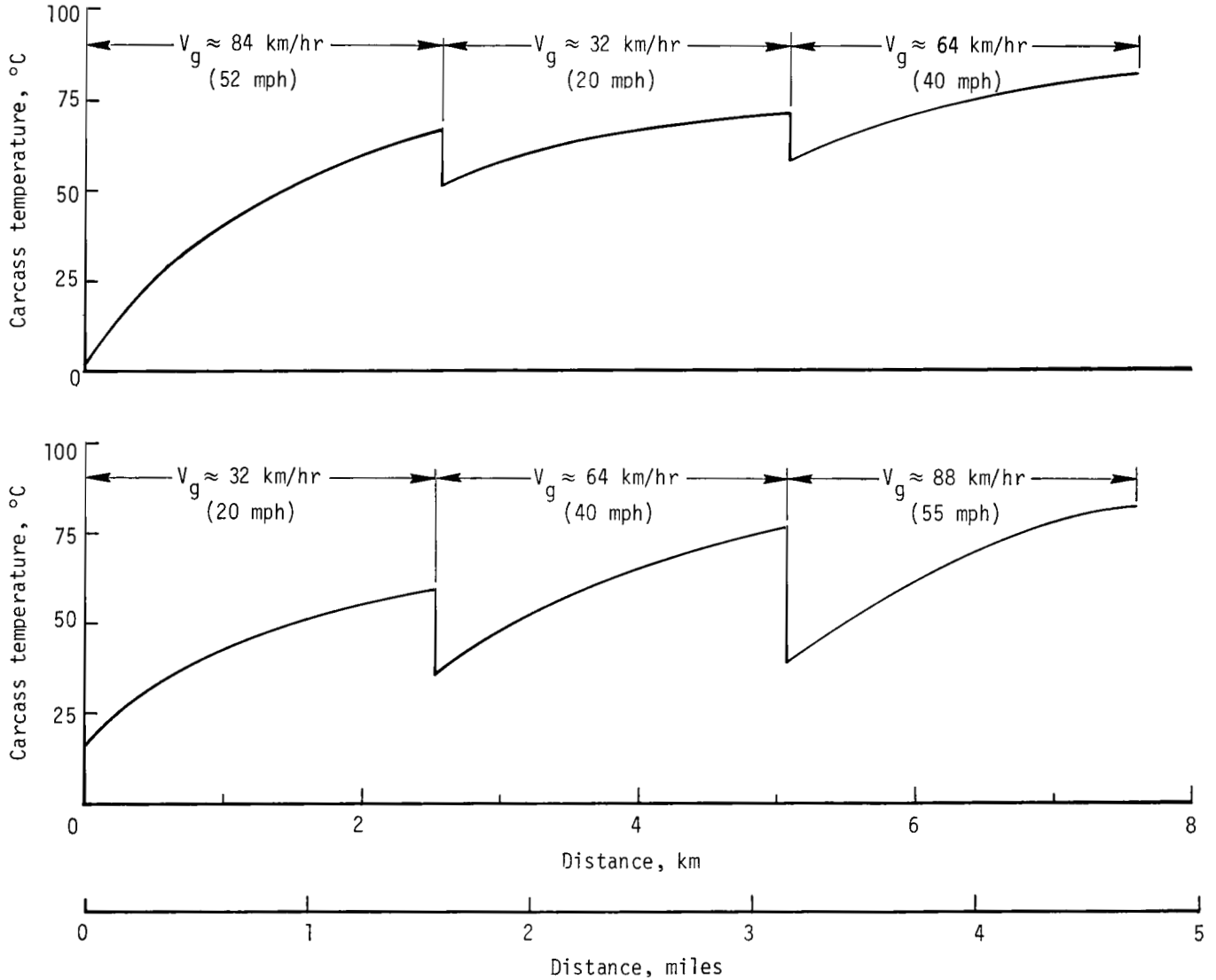

(a) Test speed.

Figure 13.- Effect of several test parameters on carcass temperature of freely rolling unyawed tire.

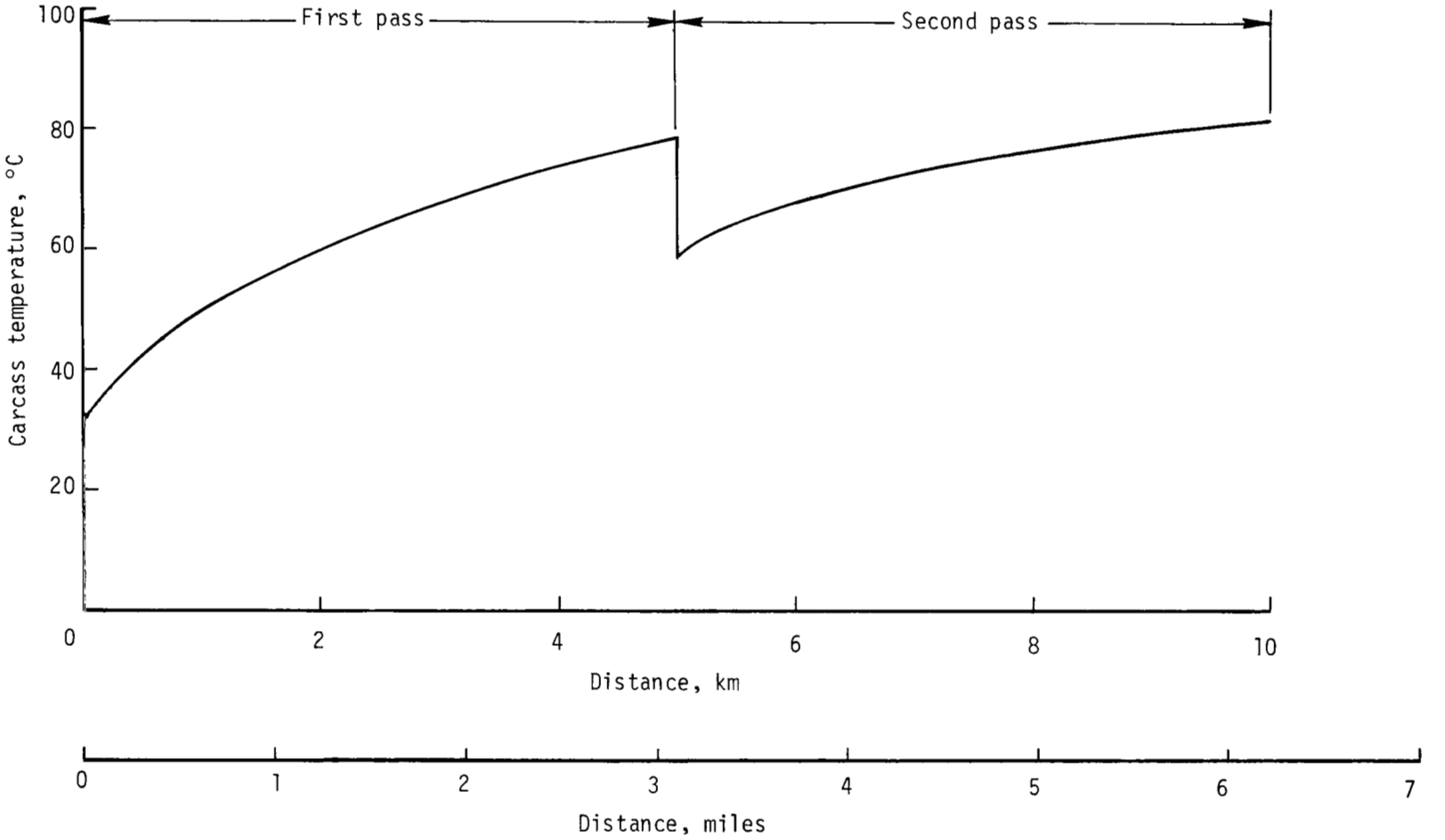

(b) Test distance.

Figure 13.- Continued.

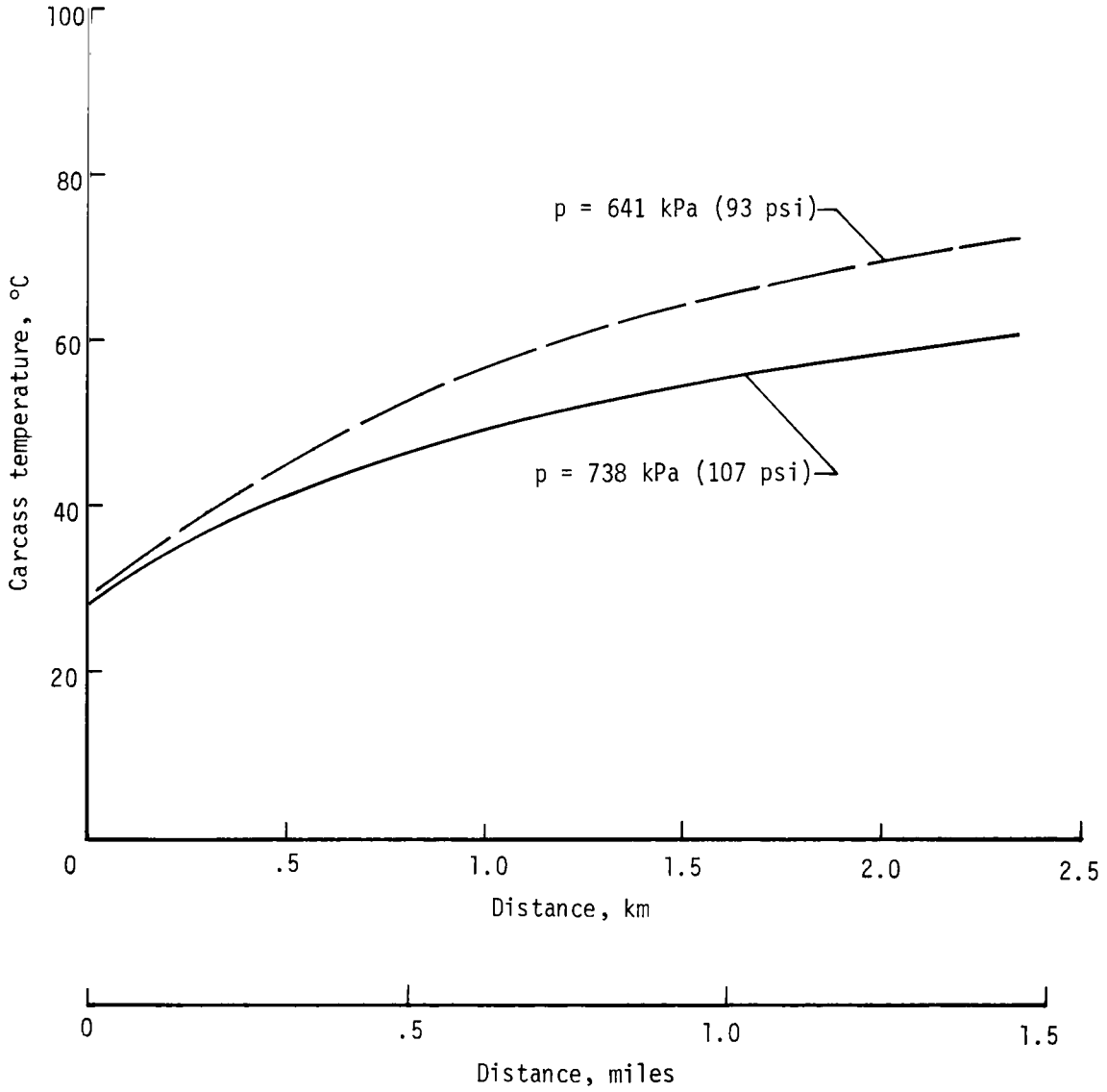

(c) Inflation pressure.

Figure 13.- Concluded.

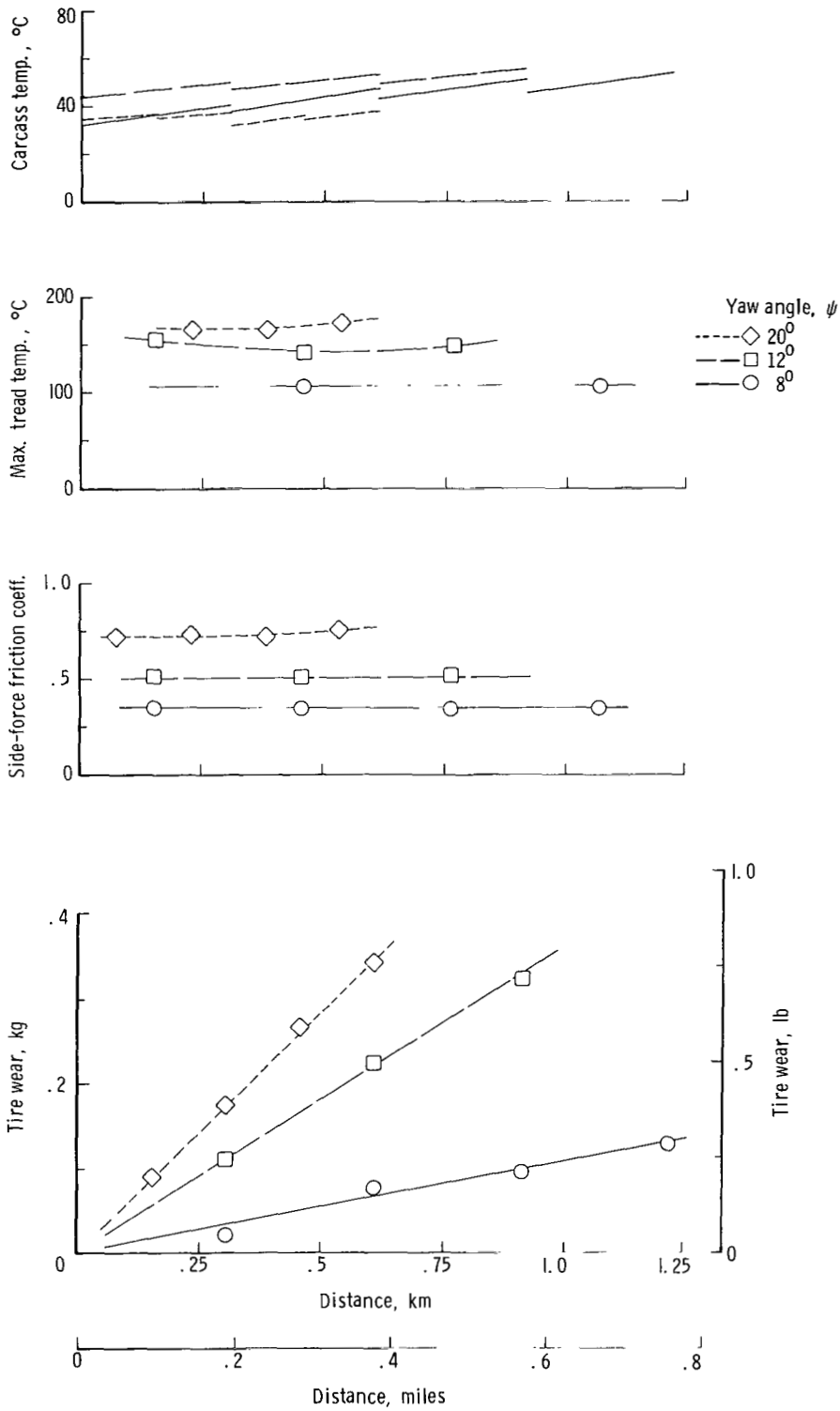

Figure 14.- Typical results from freely rolling tires at several yaw angles. Elastomer C on smooth asphalt runway surface.

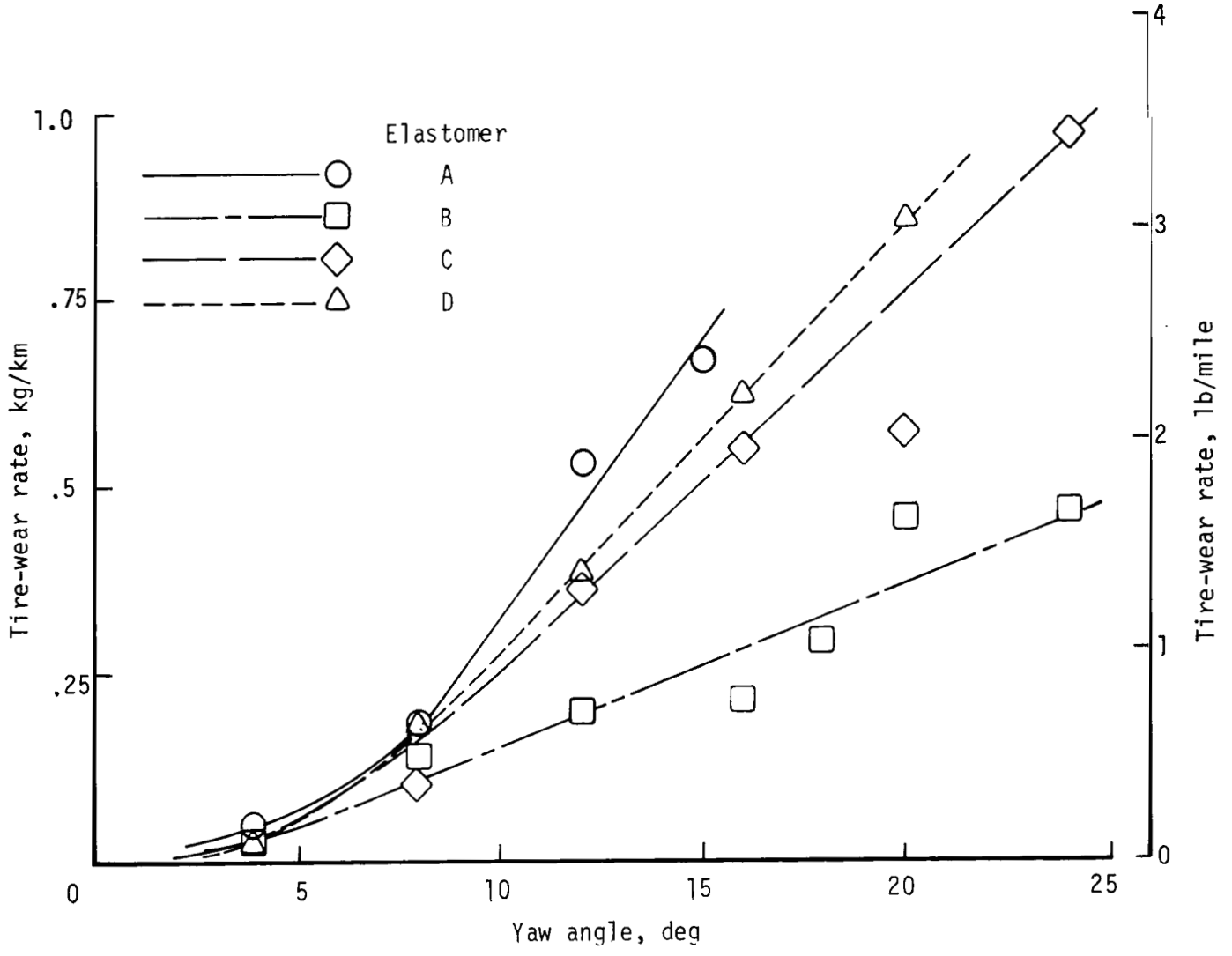

Figure 15.- Variation of tire-wear rate with yaw angle for test tread elastomers on smooth asphalt runway surface.

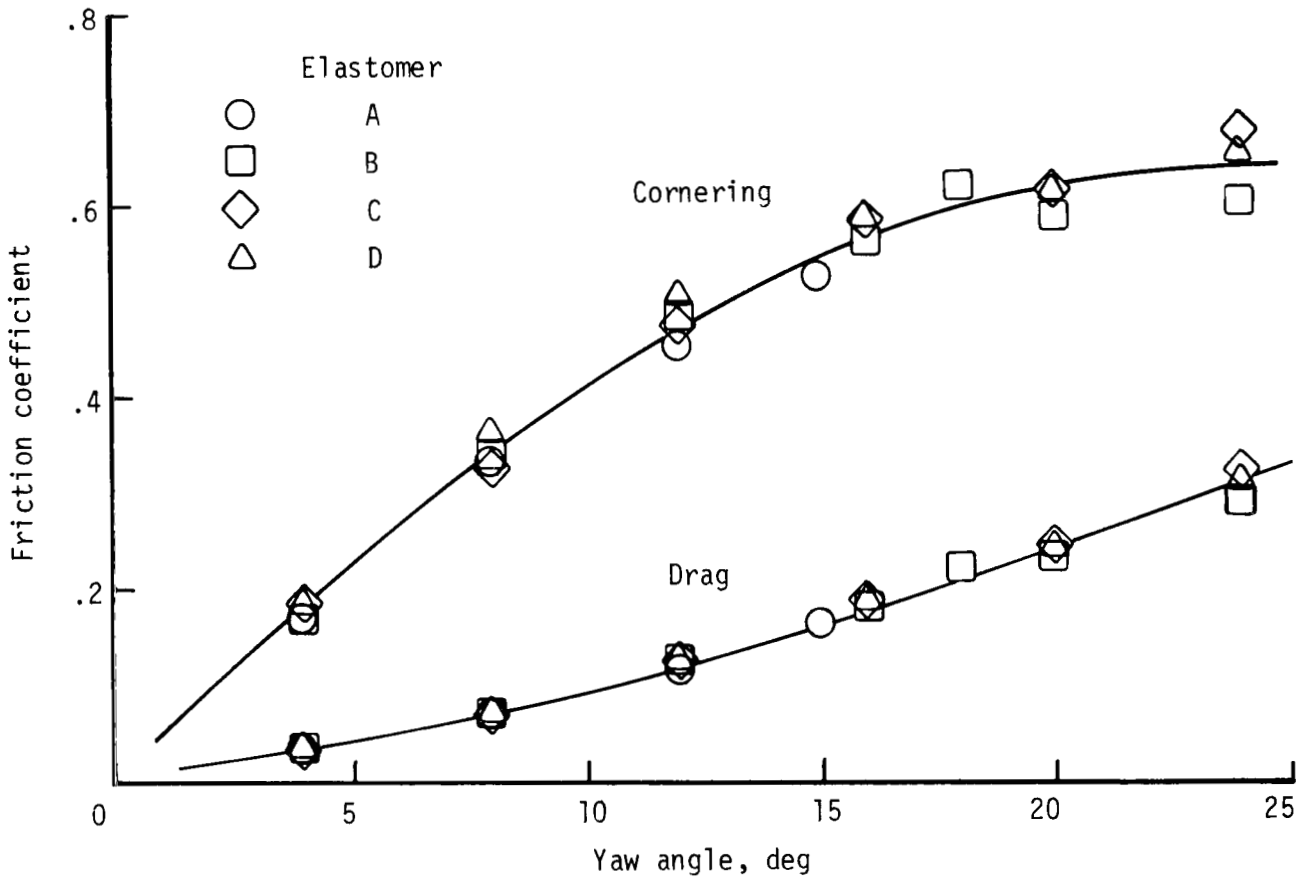

Figure 16.- Variation of cornering and drag friction coefficients with yaw angle on smooth asphalt runway surface.

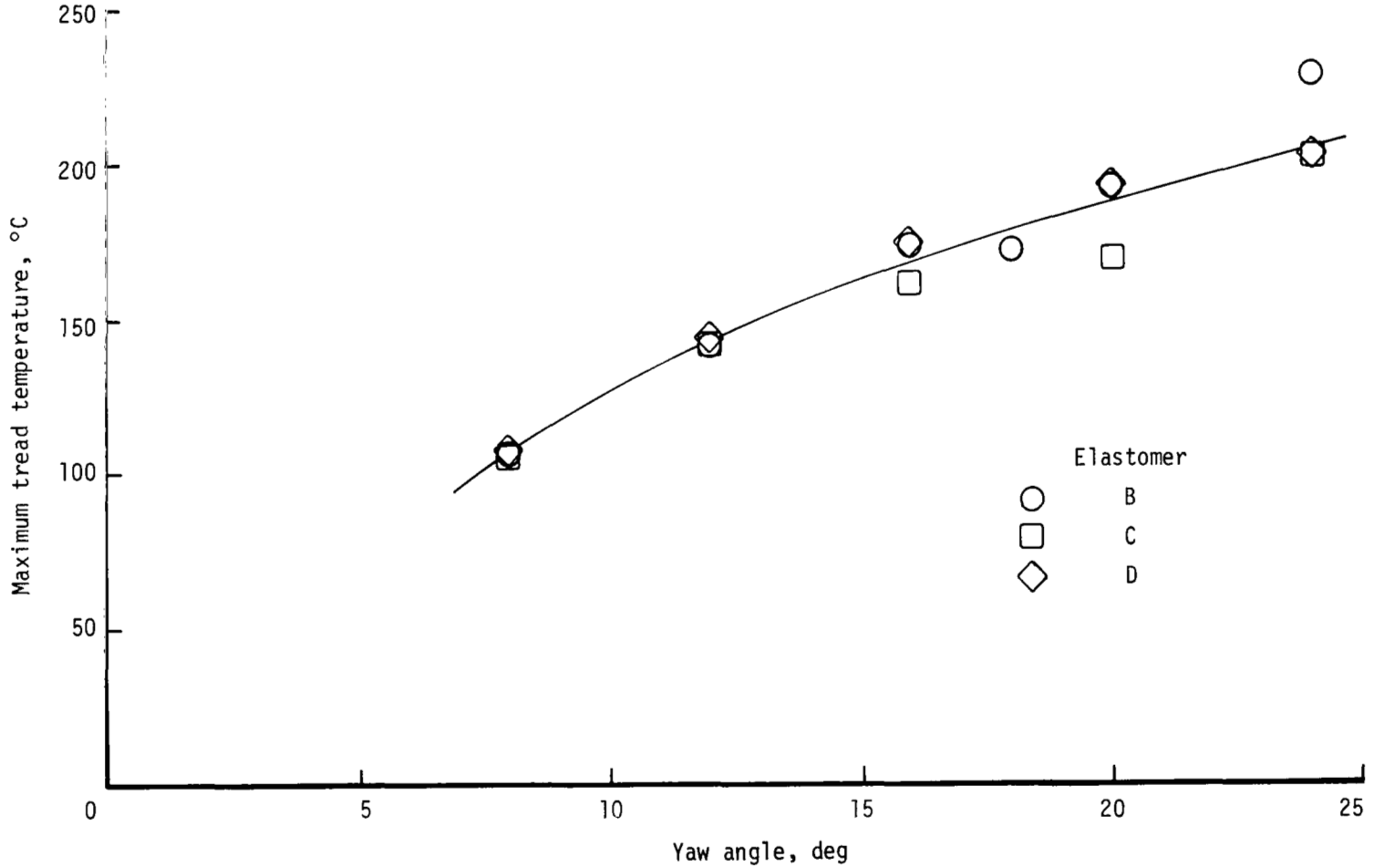

Figure 17.- Variation of maximum approximate tire-tread surface temperature with yaw angle on smooth asphalt runway surface.

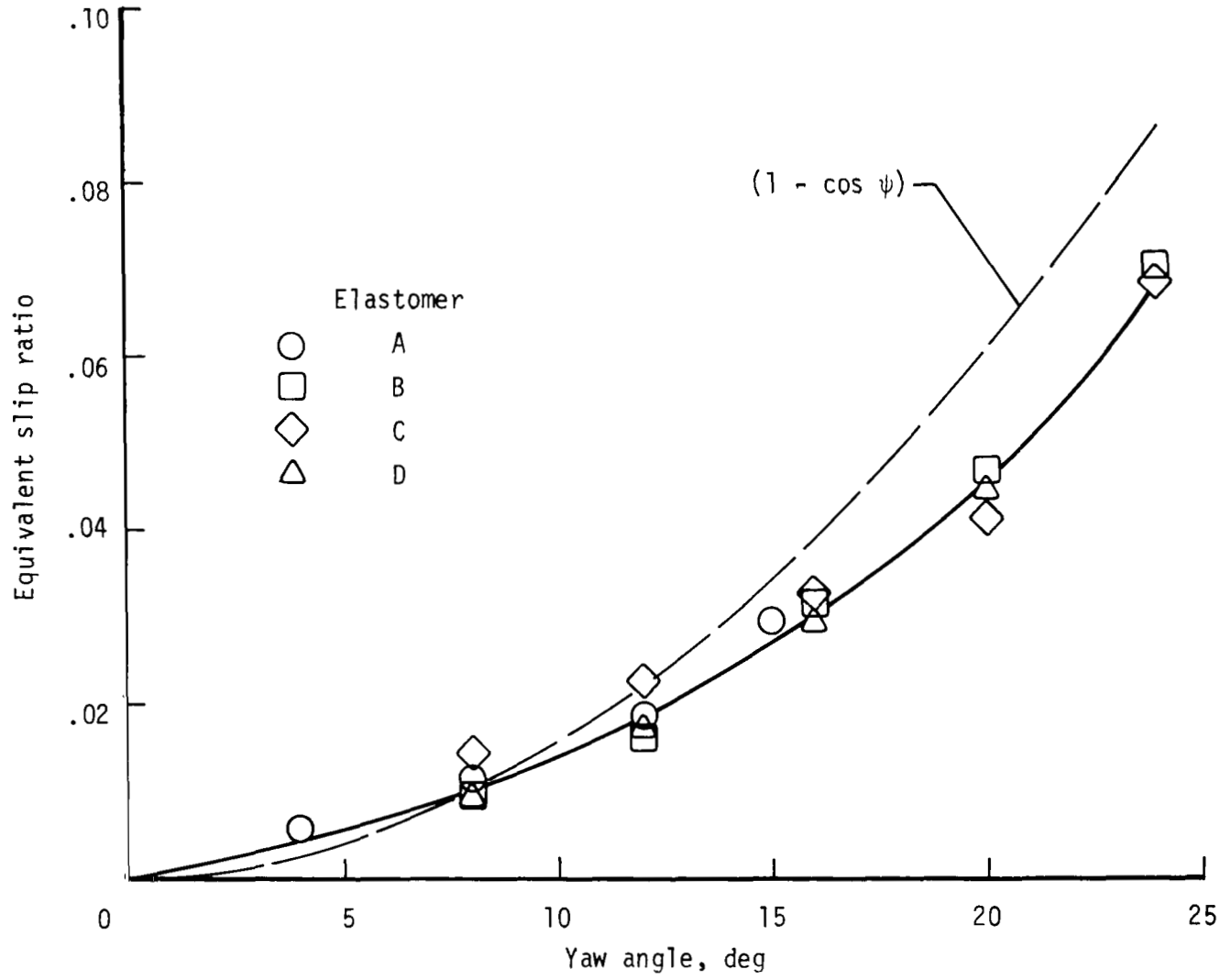

Figure 18.- Equivalent braking slip ratio from freely rolling yawed tires.

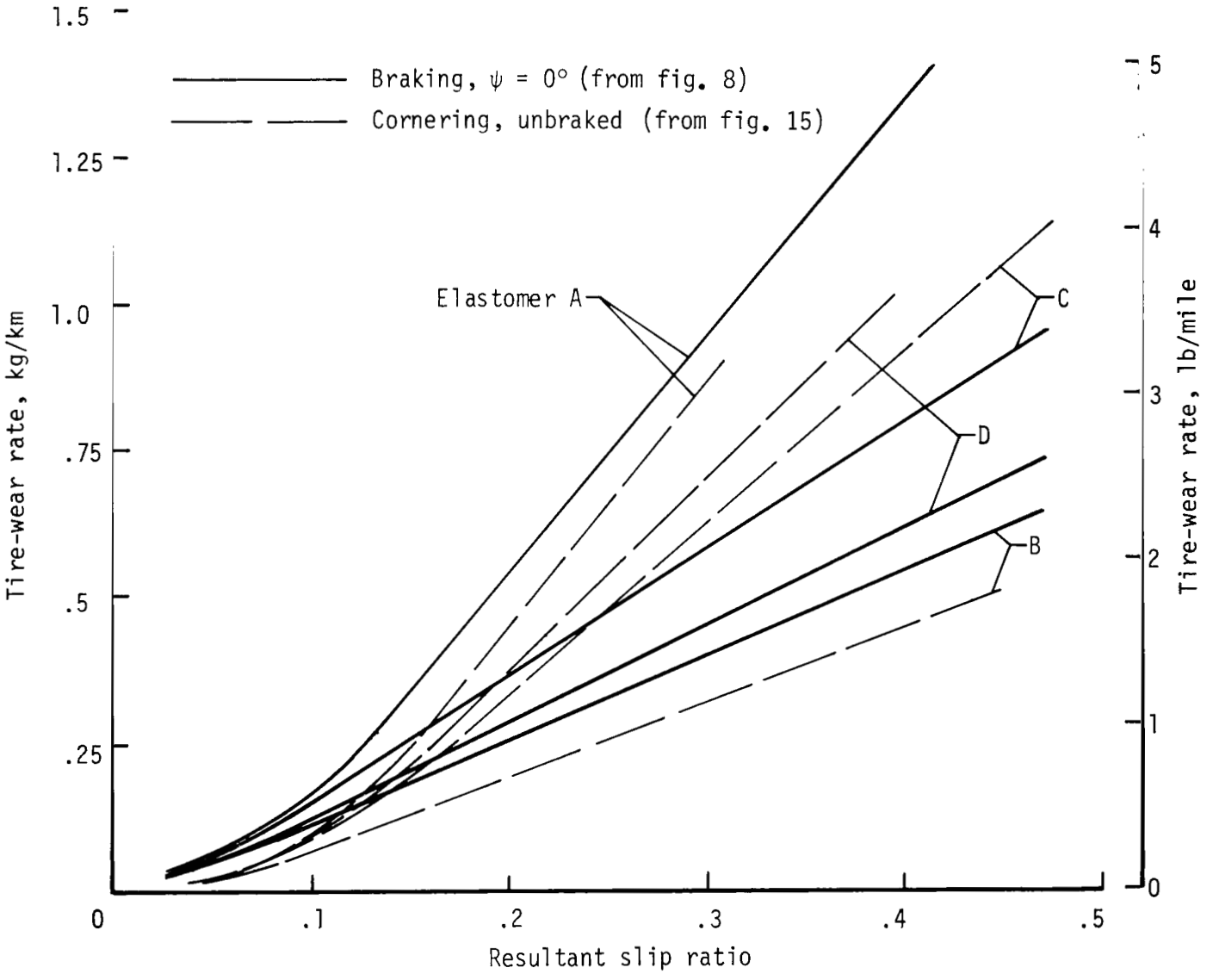

Figure 19.- Effect of operating mode on tire wear on smooth asphalt runway surface.

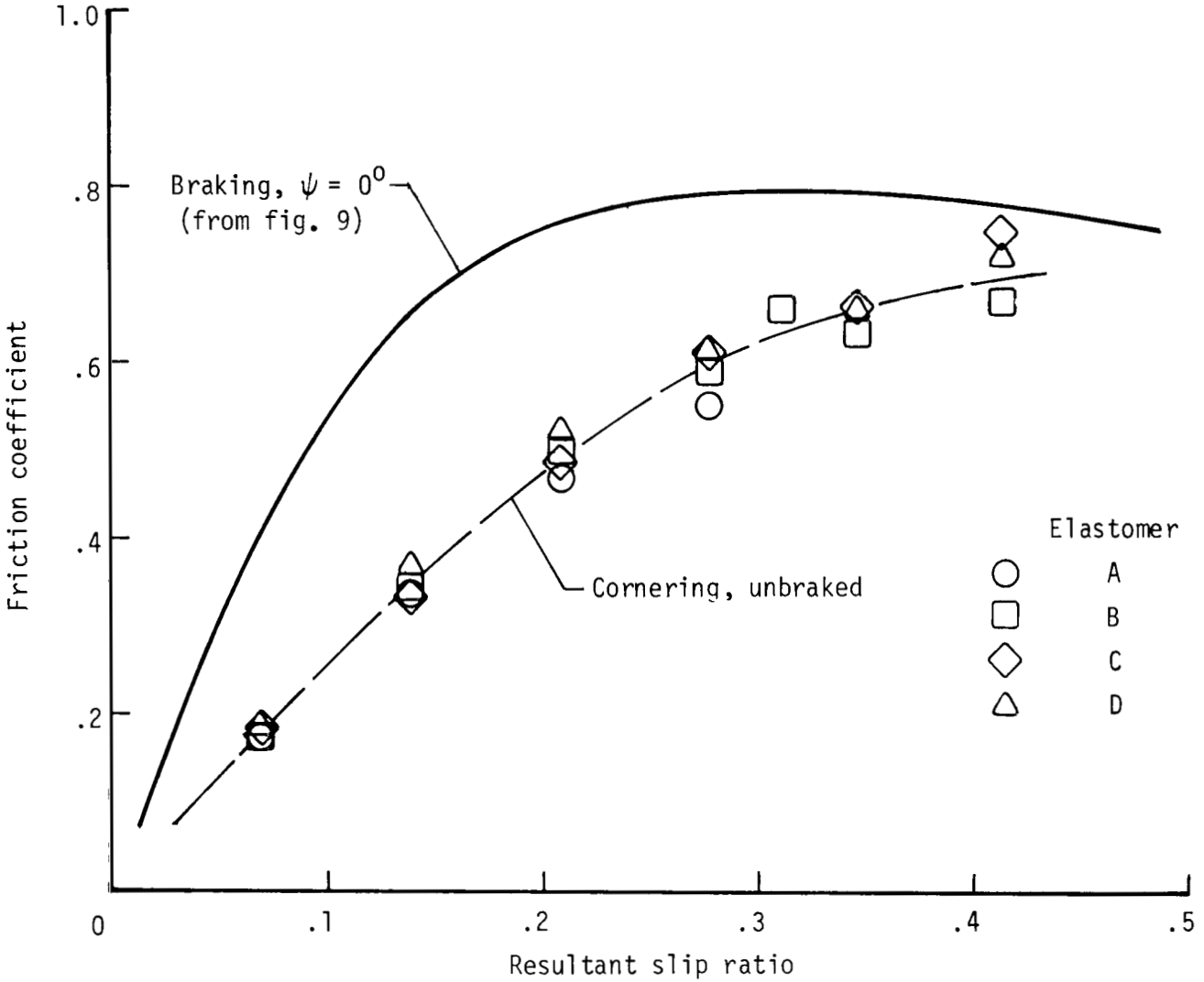

Figure 20.- Effect of operating mode on tire friction coefficient on smooth asphalt runway surface.

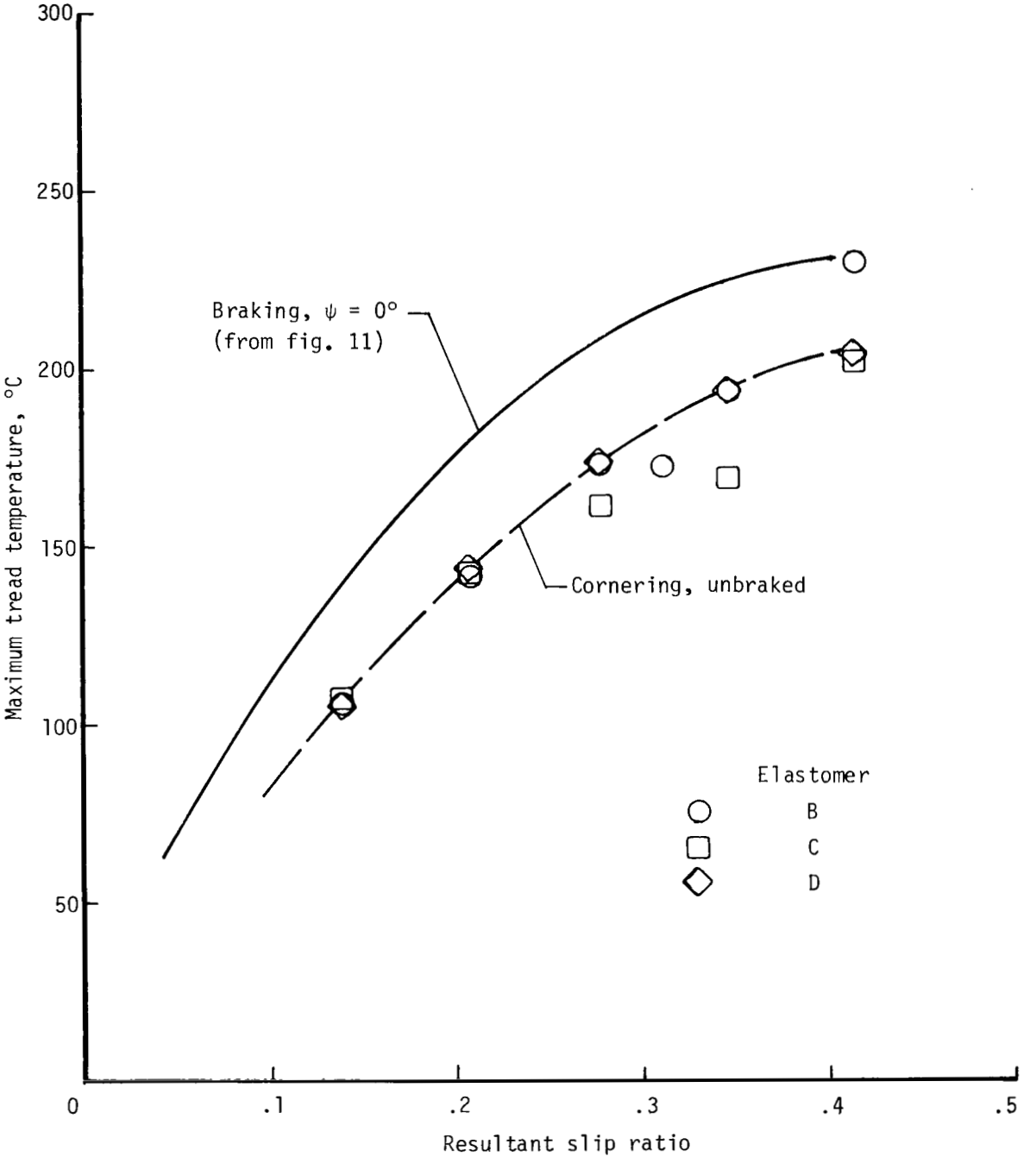

Figure 21.- Effect of operating mode on maximum approximate tire-tread surface temperature on smooth asphalt runway surface.

1. Report No.	2. Government Accession No.	3. Recipient's Catalog No.
NASA TP-1569		

4. Title and Subtitle	5. Report Date
WEAR, FRICTION, AND TEMPERATURE CHARACTERISTICS OF AN AIRCRAFT TIRE UNDERGOING BRAKING AND CORNERING	December 1979
	6. Performing Organization Code

7. Author(s)	8. Performing Organization Report No.
John L. McCarty, Thomas J. Yager, and S. R. Riccitiello	L-13239
	10. Work Unit No. 505-44-33-01

9. Performing Organization Name and Address	11. Contract or Grant No.
NASA Langley Research Center Hampton, VA 23665	
	13. Type of Report and Period Covered Technical Paper

12. Sponsoring Agency Name and Address	14. Sponsoring Agency Code
National Aeronautics and Space Administration Washington, DC 20546	

15. Supplementary Notes

16. Abstract

An experimental investigation was conducted to evaluate the wear, friction, and temperature characteristics of aircraft tire treads fabricated from different elastomers. Braking and cornering tests were performed on size 22 × 5.5, type VII aircraft tires retreaded with currently employed and experimental elastomers. The results show that the tread wear rate increases with increasing slip ratio during braking and increasing yaw angle during cornering, and the extent of wear in either operational mode is influenced by the character of the runway surface. Of the four tread elastomers investigated, 100-percent natural rubber was shown to be the least wear resistant and the state-of-the-art elastomer, comprised of a 75/25 polyblend of cis-polyisoprene and cis-polybutadiene, proved most resistant to wear. The results also show that the tread surface temperature and the friction coefficient developed during braking and cornering is independent of the tread elastomer.

17. Key Words (Suggested by Author(s))	18. Distribution Statement
Aircraft tires Tire wear Braking Cornering Ground performance	Unclassified - Unlimited Subject Category 03

19. Security Classif. (of this report)	20. Security Classif. (of this page)	21. No. of Pages	22. Price*
Unclassified	Unclassified	37	$4.50

* For sale by the National Technical Information Service, Springfield, Virginia 22161

NASA-Langley, 1979

National Aeronautics and
Space Administration

Washington, D.C.
20546

Official Business
Penalty for Private Use, $300

THIRD-CLASS BULK RATE

Postage and Fees Paid
National Aeronautics and
Space Administration
NASA-451

U.S.MAIL

4 1 1U,A, 121179 S00903DS
DEPT OF THE AIR FORCE
AF WEAPONS LABORATORY
ATTN: TECHNICAL LIBRARY (SUL)
KIRTLAND AFB NM 87117

NASA

POSTMAS S deliverable (Section 158
al Manual) Do Not Return